NEURAL PROSTHESES

1. INTRODUCTION

It is estimated that there are more than 1.3 million Americans living with some form of limb loss (1), and more than 5.4 million Americans living with paralysis (2). Together, these two groups represent more than 2% of the total US population. There are also approximately half a billion people worldwide (6–8% of the population) who suffer from disabling hearing loss (3) and over 2 million Americans living with age-related macular degeneration (AMD), which causes visual impairment (4). These statistics serve to justify the need for neurotechnologies such as neural prostheses, which are devices that can restore physiological motor functionality or sensation to users. Most recipients of a neural prosthesis suffer from damage to at least one motor or sensory pathway that inhibits their natural function (Figure 1). Whether an individual is suffering from lost limb function or the ability to see, a neural prosthesis combines physiological processes and engineering concepts to create a functional replacement.

Neural motor prosthesis control is an area of active research devoted to aiding those with lost limb function to utilize their functioning neural transmission pathways for direct control of robotic limbs (5–7). Neural prostheses that provide sensory feedback are also an active area of research ranging from restoration of hearing (8), vision (9), and touch (10). Traditional neural prosthesis examples include implants for replacing functionality in the cochlea or the retina. More recently, neurotechnology advancements have made restoring both movement and the sense of touch in upper limb amputees a reality.

In this article, we outline the building blocks and fundamental components of neural prostheses followed by in-depth discussions and scenarios of motor and sensory devices. We address the engineering and physiological challenges in both forward control and sensory feedback, and we provide examples of how novel research contributions have transformed the technology and approaches used in state-of-the-art neural prostheses. We conclude this article with a look at some of the challenges faced by current and future researchers in creating even more functional and realistic devices.

2. FUNDAMENTALS OF NEURAL PROSTHESES

The typical components of a neural prosthesis can be classified based on the purpose and function. In these devices, there is always (i) a sensor or electrode interface with the nervous system to record or output signal data, (ii) a processing unit to handle data transfer, which also includes an encoding and/or decoding algorithm to transform the data into meaningful output signals, and (iii) an interface with an external device, such as a robotic limb or sensor (Figure 2). An additional component commonly found in neural prostheses is hardware for wireless data and power transfer among the neural interface, the processing unit, and the external device or sensors. These components can be further defined based on the type of targeted neural function such as forward motor control for limb movement or sensory feedback to restore neural perceptions. The primary difference between motor and sensory prostheses is that for motor prostheses, the neural interface captures a user's intent by measuring physiological signals, but in sensory prostheses, the stimulation occurs at the neural interface to provide perception. Because of this difference, the information flow (i.e., the direction of signals) is reversed for the individual devices. In forward (i.e., motor) prosthetic devices, neural signals commonly captured by electrodes and signal conditioning circuits go from the nervous system to an external device, such as a robotic hand. In feedback (i.e., sensory) devices, a signal from the sensors on a prosthesis, such as tactile sensors, relay the sensor data back to the user's nervous system. It should be noted that in some cases sensory feedback can be sent to the processing unit for some automated control, such as in a reflex pathway to prevent object slip during grasping or even pain. Regardless, the key components of the system remain (sensor, processor, algorithm, and wireless data transfer). For bidirectional neural prostheses, specifically upper limb devices, the combination of forward control with feedback presents additional challenges for both hardware and algorithms for processing and transferring signals.

2.1. Neural Interface

In both the cases of motor and sensory prostheses, the neural interface can be at the cortical level, including cranial nerves; the spinal cord level; or peripheral level of the nervous system, each bringing their own advantages and problems. At the cortical and peripheral levels, the interface can either record from or stimulate the nervous system. An important note is that typical neural interfaces to the spinal cord aim to stimulate either motor or sensory pathways. Physiological signals for motor control are usually not recorded from the spinal cord for decoding and moving an external limb due to limitations on the ability to record signals for more than a few months using piercing microelectrode arrays (MEA) and the inability to access specific motor tracts using surface electrodes (11). However, motor pathways in the spinal cord can be stimulated to create limb movement if the corresponding pathways are still intact, such as in high-level spinal cord injury (SCI) (12, 13).

At the cortical level, electrode arrays can be placed on the surface of the scalp for electroencephalography (EEG) (Figure 3a), and penetrating MEAs can target neurons in the brain and record action potentials. One commonly used MEA is the high-density Utah slanted electrode array (HD-USEA), with up to 90 individual electrodes that can target neurons below the surface of the cortex (14) (Figure 3b). Electrodes can also be placed on the surface of the brain directly for electrocorticography (ECoG) (15) (Figure 3c). While EEG arrays are typically used for recording population signals from the brain, ECoG and

J. Webster (ed.), *Wiley Encyclopedia of Electrical and Electronics Engineering*.
DOI: 10.1002/047134608X.W1424.pub2

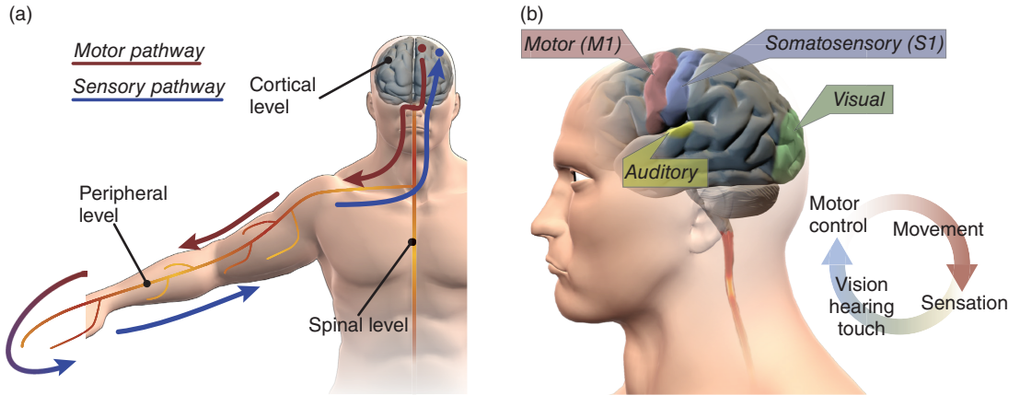

Figure 1. The human nervous system contains both motor and sensory pathways. (a) Voluntary body movement intent originates at the cortical level and then descends through the spinal cord and peripheral nerves to muscles. Sensory receptors throughout the body capture external information and provide feedback through ascending pathways. (b) At the cortical level, motor and sensory information is represented in different cortices of the brain. For neural prostheses, the primary motor cortex (M1) is of interest for accessing and decoding intended movement, while somatosensory (S1), visual, and auditory cortices contain regions for accessing and encoding feedback. Together, the motor and sensory pathways form a continuous cycle of feedback to improve efficiency and functionality in our daily lives.

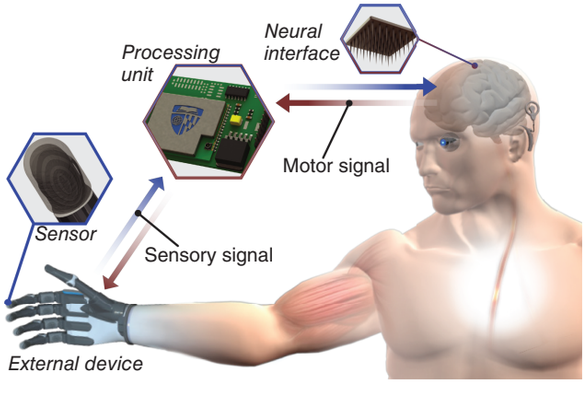

Figure 2. The fundamental components of neural prostheses include a neural interface, a processing unit to interpret the signal, and an external device such as a prosthetic hand with a touch sensor. Together, these make up the neural prosthesis, which connects to the nervous system and aims to restore motor, sensory, and even cognitive functionality. Common devices include cochlear implants, visual prostheses, and prosthetic limbs. Whether providing sensory perception (vision, hearing, touch, etc.) or forward control (limb movement), a neural prosthesis can have a significant impact on improving functionality. The external device can provide movement (motor prosthesis) or be a sensor for capturing perception (sensory prosthesis). A bidirectional neural prosthesis, such as a prosthetic arm, includes pathways for both feedforward control and sensory feedback to the user's nervous system.

penetrating MEAs can be used for stimulating or recording from neurons. In the spinal cord, epidural stimulation using surface electrodes is often used to manage pain, but this technique can also be used to elicit limb movements (12). Microwires and penetrating MEAs can also be used to stimulate the spinal cord for providing motor movements in intact limbs (12) or for activating afferent neurons for sensory feedback (18). Microwires, nerve cuffs, penetrating microelectrodes, and noninvasive electrodes on the surface of the skin can be used for interfacing with the peripheral nervous system (PNS). At the peripheral interface, the electrodes can be used to record muscle activity from electromyography (EMG) for motor control or to stimulate peripheral nerves for sensory feedback (Figure 3d). In addition to cuff electrodes that wrap around and stimulate an entire peripheral nerve (Figure 3e), there are also specialized electrodes for sensory feedback, namely the longitudinally implanted intrafascicular electrode (LIFE), which penetrates the nerve to target a single fascicle (19) (Figure 3f); the transverse intrafascicular multichannel electrode (TIME), which penetrates the nerve and targets multiple fascicles (16) (Figure 3g); and the flat interface nerve electrode (FINE), which increases the surface area of target fascicles and moves central axons within the fascicle closer to the surface of the nerve (20).

More recently, novel electrode designs, including split rings and flexible ribbons, have been developed to provide better access to the peripheral nerves (17, 21) (Figure 3h). Researchers have also created microwire electrodes using carbon nanotube yarns to achieve diameters of 10 μm, making them suitable for reducing nerve damage and inflammation due to their small size as well as interfacing with small nerve bundles (100–300 μm) (22). Advances in materials have led to neural interfaces that are conformal and biocompatible to help reduce inflammatory responses (23). Electrodes have also been developed that are smaller, more dense (24), and more flexible (25). Although we provide a brief introduction in this article, a more detailed discussion of electrodes for neural interfacing, including material considerations, can be found in (26, 27), and a review of implantable technology for stimulation can be found in (28).

Sensory feedback through the neural interfacing can be achieved using either constant voltage or constant current stimulation strategies (29); however, it is worth

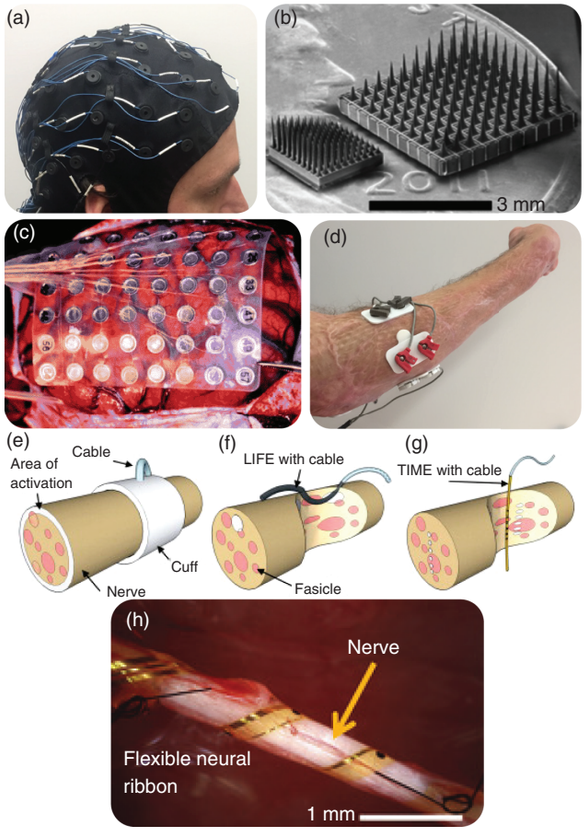

Figure 3. Modalities for neural interfacing. (a) EEG electrodes for noninvasive recording from the scalp. (b) Penetrating high-density Utah slanted electrode array (HD-USEA) used for recording or stimulating at cortical, spinal cord, and peripheral levels. Source: Reproduced from (14) under the Creative Commons Attribution (CC-BY) license. (c) ECoG electrode array for cortex-surface recording or stimulating. Source: Reproduced from (15) under the CC-BY license. (d) Surface electrodes for measuring EMG or providing transcutaneous peripheral nerve stimulation. EMG signals can also be obtained intramuscularly using implanted fine wires. (e–h) Electrodes for peripheral nerve stimulation. (e) Standard cuff electrode wrapped around a nerve, (f) a LIFE activating a single fascicle within the nerve, and (g) a TIME activating multiple fascicles within the nerve. Source: Reproduced with permission from (16), © 2010 Elsevier. (h) More recent developments have led to flexible stimulating electrode that can wrap around a nerve bundle. Source: Reproduced from (17) with permission from Wiley, © 2015 WILEY-VCH Verlag GmbH & Co. KGaA, Weinheim.

noting that mechanical stimulation can also be provided to peripheral nerves to elicit sensory feedback as we will discuss in more detail later (30). More recent approaches to neural stimulation also include optical (31) and optogenetic techniques to provide sensory feedback (32) and stimulate motor neurons in the PNS (33) and CNS (34). A more thorough discussion of these optical stimulation techniques can be found in (35). An overview of the type of signals captured by the various neural interfaces discussed in this section can be found in (36).

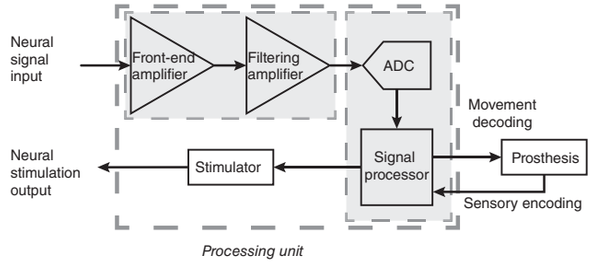

Figure 4. General system block diagram for a neural prosthesis, including forward motor control and sensory feedback. The processing unit contains elements for signal amplification and filtering, wireless data transfer, decoding and encoding algorithms, and an interface to external devices and sensors.

2.2. Processing Unit

The processing unit of a neural prosthesis is made up of several key components including signal amplifiers and filters, an analog-to-digital converter (ADC), a signal processor or microprocessor, and encoding or decoding algorithms for interpreting neural and sensor signals (37) (Figure 4). For this article, we will also consider hardware for wireless data and power transfer between the processor and external devices, such as a robotic arm or implanted electrodes, as part of the processing unit. A neural signal requires specifically designed biopotential amplifiers and filters because the bandwidth and amplitude of a neural signal depend on the electrode type being used (i.e., EEG, ECoG, EMG, and spikes) as well as the location of biopotential acquisition, but, in general, neural signals require amplifiers with high gain and low noise (38). The hardware for stimulation can be thought of as a component within the processing unit, although they may be separated physically.

2.2.1. Wireless Data and Power Transfer. There is no explicit requirement for wireless data and power transfer, but it is common for the external device or sensor to be physically detached from the processing unit. However, a major benefit of wireless data and power transfer is that the physical detachment of systems can help reduce infection by avoiding breaking the skin with penetrating wires. Wireless protocols such as Bluetooth allow data transfer between a central processing unit and external devices such as robotic arms, sensors, or a PC. Wireless protocols impose limits on data transfer bandwidth while also requiring additional power considerations. Neural implants with wireless data transfer often rely on implanted power sources and communicate with non-implanted processing units with external power supplies (39). For smaller implants or devices with less power requirements, wireless power transfer is a viable option to eliminate the need to implant a power source. An example of this is the cochlear implant where an external microphone is placed outside of the body on or behind the ear, and a wireless connection is made through the skull to an implanted receiver, microprocessor, and stimulator (8). In a cochlear implant, the stimulator is powered wirelessly using a magnetically coupled coil pair with

the transmitting coil in the external unit. This near-field resonant inductive coupling (NRIC) strategy utilizes electromagnetic induction and is one of the most common and widely used methods of wireless power transfer. Other examples of wireless power transfer include near-field capacitive coupling, which works based on two conductors and electric field coupling (40). Another strategy using ultrasonic energy transfer enables wireless power transfer to implants a few centimeters away (41), whereas more recent mid- and far-field wireless power transfer strategies can power microimplants up to 5 cm away, but not without limitations on the amount of power being supplied (i.e., <5 mW) (42, 43). For a full review and discussion on wireless power transfer strategies for implants, see Reference 44.

2.2.2. Encoding and Decoding Algorithms. The encoding and decoding algorithms for a neural prosthesis, which are part of the signal processor in Figure 4, are crucial for the functionality and efficacy of the system. Algorithms can be designed to determine intent (i.e., decode), such as limb movement, or they can transform a sensory signal (i.e., encode), such as touch, to be passed back to the user's nervous system. In either case, the algorithms are implemented either in the software directly on a microprocessor or PC, or in the hardware as customized circuits. Most neural prostheses utilize a microprocessor PC for decoding and encoding algorithms due to increased flexibility and ease of implementation. However, an example of hardware implementation is a spike detection algorithm based on changes in neural signal energy above noise levels (45). Another example is a neurostimulation array with on-chip current steering and charge balancing (46). For a more thorough review of very-large-scale integration (VLSI) circuit implementations for neural systems, see Reference 47.

2.3. External Hardware Interface

The final fundamental component of a neural prosthesis is the external hardware. For motor prostheses, the external hardware is typically a robotic limb, a cursor on a screen, or a wheelchair controller. In the feedforward case (i.e., motor prosthesis), the external hardware is the component that carries out a user's intent (i.e., movement). For a sensory prosthesis, the processing unit connects to and processes signals from external sensors. The sensors in the feedback case (i.e., sensory prosthesis) capture parts of the environment, such as the sense of touch, which is transmitted back to the user (i.e., sensory perception). Examples of sensors include microphones in cochlear implants, cameras for retinal prostheses, or force sensors in a robotic hand. The external hardware is crucial to a neural prosthesis because it is the interface between the environment and the user. In both the cases, the external hardware also interfaces with the processing unit and the decoding/encoding algorithms.

For bidirectional neural prostheses, the external hardware contains both motor and sensory elements. One real-world example is the modular prosthetic limb (MPL) by the Johns Hopkins University Applied Physics Laboratory (JHU/APL) (48) (Figure 5a). The MPL is capable of mimicking almost every movement of a human arm. It is a sophisticated robotic limb and has been the external hardware used in several key developments for motor neural prostheses (49–51). In addition, the MPL contains force, acceleration, torque, temperature, and position sensors (Figure 5b). The MPL has also been used as a sensory prosthesis wherein tactile measurements from sensors in the hand were used to stimulate the primary somatosensory cortex (S1) in both humans (52) and nonhuman primates (53) to provide realistic sensory feedback.

3. NEURAL MOTOR PROSTHESIS

The volitional aspects of human movement produce electrical activity within the somatic nervous system from the sensorimotor cortex to neuromuscular junctions throughout the body. By recording electrical activity within this system, the consequent signal patterns are extracted and leveraged to infer specific movement intentions. Such inferences, often achieved with pattern recognition and machine learning algorithms, are then used to activate a robotic prosthesis in a way that is consistent with the user's intention and intuition.

3.1. Methods of Neural Recording

There is a topographic organization (spatial mapping) in the brain defined by columns of neurons, which are

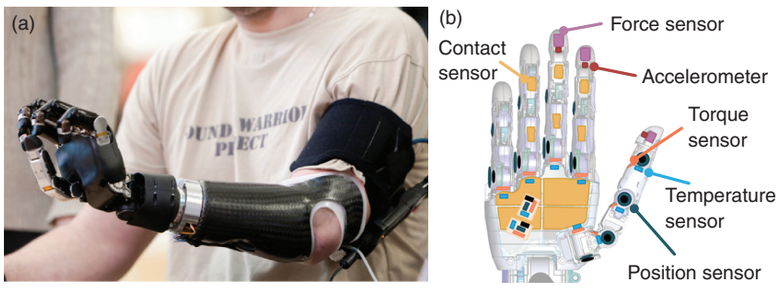

Figure 5. (a) The JHU/APL Modular Prosthetic Limb has 26 controllable degrees of freedom in 17 articulating joints. (b) Over 100 sensors including position, force, acceleration, contact, and temperature. Source: Images courtesy of Johns Hopkins University Applied Physics Laboratory.

tuned to different sensorimotor cortical signals (54, 55), and more recently have been extensively delineated (56). This spatial mapping enables the recording of regionally specific and decipherable information about sensorimotor inputs and outputs from electrodes placed over populations of neurons. The interactive components of neural recording, stimulation, and signal interpretation are collectively referred to as brain–computer interface (BCI) or brain–machine interface (BMI).

The BCI community has explored different techniques to access and record neural signals, but four modalities are dominant (36): (i) *EEG*, measuring neural potentials from the cortex with noninvasive electrodes placed on the scalp; (ii) *ECoG*, measuring cortical potentials from the surface of the cortex; (iii) *action potential recording*, measuring single-unit, multiunit, or population and local field signals through direct cortical penetration using MEA; and (d) *EMG*, measuring accumulated potentials of neuron motor units firing within the muscle tissue. Although EMG is not strictly a neural signal, the muscle tissues serve as surrogates or amplifiers of peripheral nerve signals for motor interfacing. Each signal modality has distinct characteristics, strengths, and weaknesses which are discussed in the following sections (Figure 6).

3.1.1. Electroencephalography (EEG). Owing to its minimal invasiveness, high temporal resolution, and relatively low financial cost, EEG has become one of the most studied neural recording methods. A typical EEG sensor network is composed of 64 or 128 common-reference monopolar electrodes uniformly placed along the scalp, though the quantity and type of electrodes can vary (Figure 3a). To improve contact and conduction, electrolytic gel is often applied at the point of body-electrode contact. There are three primary features extracted from the EEG signals for neural control: steady-state visually evoked potentials

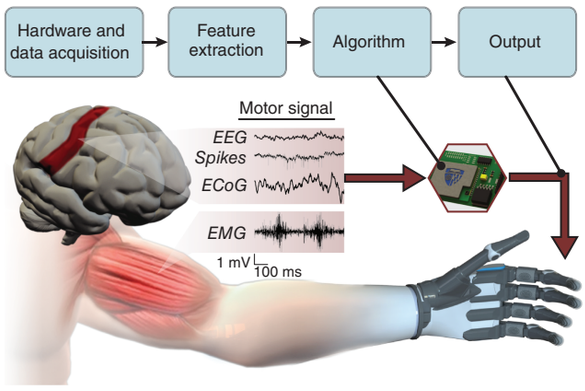

Figure 6. Motor neural prostheses utilize neural signals that convey user intent. One example is decoding EMG signals to determine the intended movement of a hand prosthesis. The primary motor cortex (M1) can be recorded to capture neural activity in the form of EEG, neuron spikes, or ECoG signals. EMG signals from the peripheral nervous system (PNS) can also be used to capture motor intent. The motor signal is processed to extract key features before passing through an algorithm to determine the desired movement.

(SSVEP), P300 response, and event-related desynchronization (ERD)/event-related synchronization (ERS). SSVEP refer to a phase-locked modulation in the EEG signal in response to visual stimuli flashing between about 5 and 75 Hz. The SSVEP has been used for BCI control by enabling users to select among multiple options on a computer screen (57). P300 refers to delayed increase in smooth-signal amplitude responding at around 300 ms after observing an anticipated event. The P300 feature has been used to select desired alphabetic letters for spelling tasks in nonverbal communication (58). ERD and ERS refer to complex alterations such as spectral power or entropy changes occurring in the brain rhythm from the motor cortex area during intentions to initiate movement. ERD and ERS, in addition to other features extracted from raw EEG signals, have been used to decode one-, two-, and, in rare demonstrations, three-dimensional hand movements (59).

EEG signals are subject to a range of interference mechanisms. The intervening cranial tissues between the EEG recording electrodes and the neural signal sources create a low-pass filtering effect on the signals. EEG signals are recorded from dense populations of millions of neurons firing rapidly, and much information relevant to motor intent are found at higher, gamma band (70–150 Hz) frequencies (50). The low-pass filtration serves to block much of the spatial and temporal information of interest and, consequently, EEG is generally considered to be a poor method for recording frequency information above 70 Hz (60). Acquiring useful information from EEG signals can be further complicated by unpredictable changes in the skin-electrode contact due to head movements. The spatial resolution of EEG remains limited but can be increased up to a point by changing the density of EEG electrodes across the scalp (50). Therefore, more invasive approaches such as electrocorticography are available, which place the recording electrodes on the brain surface to obtain greater specificity.

3.1.2. Electrocorticography (ECoG). ECoG generally represents a middle ground between EEG and penetrating MEAs. ECoG yields more spatially detailed information than EEG, but electrode measurements cover a wider area than MEAs. ECoG signals are recorded from platinum disk electrodes placed directly on the cortex surface, but do not penetrate the cortex itself (Figure 3c). ECoG recording can be performed with a variety of electrode sizes and spacings, allowing greater selectivity over spatial resolution and surface coverage. A common average reference (CAR) filter is typically applied to the raw ECoG signals to remove signal activity, which is common among all recording electrodes (61, 62). After CAR filtration, signal features are extracted as physiologically relevant frequency bandwidths (μ: 7–13 Hz, β: 16–30 Hz, low γ: 30–50 Hz, high $\gamma 1$: 70–100 Hz, and high $\gamma 2$: 100–150 Hz) (Figure 7).

Though many of the signal features extracted from ECoG can yield information about movement intentions, some are empirically superior for movement decoding. For example, μ-band content contains movement-related information (65), but the required signal smoothing may

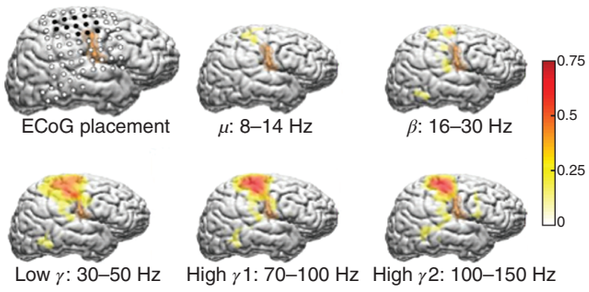

Figure 7. ECoG spatial and frequency distributions and correlations of actual and reconstructed grasp aperture for reach-to-grasp movements. High γ bands can be used to provide good performance for neural prosthesis motor control (50, 63, 64). Source: © 2011 IEEE. Reprinted, with permission, from (62).

create a time delay that is too great for a real-time movement decoding scheme. The μ and β frequency bands tend to decrease in power during movement; however, the spatial distribution of this phenomenon across the cortex may be too broad to encode specific movements (66). The high γ-band, which correlates to the firing rate of local neuron groups (67), provides relatively precise information about specific movements (68). As a result, the high γ-bands have been used as features to decode reaching and grasping kinematics during upper arm movements (50, 63, 64). Furthermore, these signals have been used to control a robotic arm with three degrees of freedom (69, 70).

3.1.3. Action Potential Recording. The difficulties in acquiring information of interest from EEG have led to the use of invasive electrodes such as MEAs capable of measuring highly localized neural information from direct cortical penetration (Figure 3b). Action potentials or *spikes* resulting from the firing of individual neurons can be extracted from raw signals recorded with MEAs in order to drive or intuitively activate a robotic limb (71, 72). MEAs capture signals from neurons, either singly (from a single unit or neuron) or multiply (from multiple units or neurons). By their proximity, the single and multi-unit signals purport to provide greater specificity in their encoding of motor information. In contrast, local field potentials (LFP) are recorded extracellularly, capturing more filtered, lower frequency signals, and they provide a more general representation of the activity in a given population of neurons. LFP can be further decomposed with signal-processing methods into individual frequency bands to determine ERD and ERS features corresponding to different motor actions. The recorded LFP and ERD/ERS can thus be decoded in order to give paralyzed patients control of a robotic limb (73) of up to 10 degrees of freedom (74).

MEAs yield signals with high spatial and temporal resolution; however, this type of neural recording has a number of drawbacks. Owing to small physical size, MEAs record action potentials from a limited area of the cortex, which may not fully represent the neural activity of interest. Furthermore, chronic MEA penetration of the cortex causes an immune response called *gliosis*, which degrades the recording quality over time (75–77). Gliosis is a central nervous system response to acute injury (e.g., cortical penetration) wherein glial cell proliferation can lead to axonal inhibition and degeneration. Additionally, MEA spike recordings are quite sensitive to motion in the electrode recording sites. This electrode movement can cause dropout in the recording of individual neurons, altering the ability of movement-intent decoding algorithms to interpret the MEA signal. As a consequence, these decoding algorithms must be frequently retrained (51).

3.1.4. Electromyography (EMG). To perform a voluntary body movement, neural signal patterns encoding the movement are transmitted from the motor cortex along motoneuron axons to various peripheral neuromuscular junctions embedded within specific muscles. The collective electrical responses, or EMG signals, delivered to the muscles at these junctions control muscle contractions and effect the desired movement. Victims of paralysis may have little or no motor control, requiring one of the direct neural interfaces mentioned previously. However, for amputees, EMG from muscular contractions in the residual amputated limb can be used for prosthesis activation (78). Such an activation method is called *intuitive* when the prosthesis limb output response from a given muscle contraction pattern corresponds to the expected intact limb behavior resulting from a similar contraction.

EMG can be recorded invasively with implanted electrodes measuring local intramuscular activity, or with skin-surface contact electrodes measuring more regional muscular activity (Figure 3d). Furthermore, the information content obtained from EMG signals can be enhanced with targeted muscle reinnervation (TMR), a surgical technique to repurpose healthy muscle tissue near the amputation site by redirecting nerves that originally served the now-amputated limb (79). When using EMG for prosthesis activation, typically, bipolar electrodes pairs are placed to record activity from healthy muscles nearest the point of amputation. To amplify the signal of interest while minimizing signal corruption from body movement, raw EMG signals are often bandlimited to roughly 25–450 Hz. There are a number of features extracted from the filtered EMG signal, which have proven useful for prosthesis activation: mean absolute value, waveform length, variance, and zero crossings (80); autoregressive coefficients (78); and the discrete-time Fourier transform (81, 82). EMG has emerged as the most common neural motor prosthesis interface due to relatively inexpensive hardware, minimal invasiveness, and an established empirical track record as a reliable signal for prosthesis control.

3.2. User Intention Decoding and Prosthesis Activation

3.2.1. Pattern Recognition and Machine Learning. The neural activity or muscle contractions involved in performing certain limb movements can generate unique and reproducible patterns in the recorded neural signals. The key to movement intention decoding for intuitive neural prosthesis control is to first convert the signals

into useful data structures, a process known as feature extraction, and then to map patterns in the extracted signal features to their corresponding output motions using pattern recognition or machine learning tools. For example, machine learning tools such as neural networks (83), linear discriminant analysis (84), support vector machines (85), maximum likelihood estimation (86), and the Kalman filter (87) have been used to classify distinct upper limb movements from neural signal features. The general movement decoding framework is largely the same irrespective of neural recording modality or the machine learning techniques utilized, but approaches can differ based on a variety of factors such as the relevant features extracted from each neural signal, the algorithmic properties of the machine learning tool, and the level of control sophistication obtainable from the signal of interest. Selection of an appropriate machine learning algorithm among innumerable choices can be based on many factors ranging from the desired algorithmic properties to, quite simply, personal preference.

The mapping of signal patterns to movement output predictions is done through a training process wherein a human subject will attempt to perform or mimic a range of desired output movements while neural signal data are collected. A person with lost limb function is, by definition, physically unable to fully perform the movements. Therefore, the neural signals collected indirectly represent the person's intent or volition via electrical activity produced in the motor cortex, or in the case of amputees and TMR patients, muscle contraction activity from EMG. Owing to the lost limb function, there is currently no way to objectively confirm during the training process that the measured signal patterns are correctly mapped to a subject's desired corresponding movement intentions or targets. As a result, much care is taken to help ensure this synchronicity, which typically involves a qualified clinician or prosthetist guiding the subject through a structured and repetitive training process further reinforced by visual movement cues. For example, a computer terminal can be used to present a three-dimensional representation of the desired movement(s), and the clinician will instruct paralyzed subjects to simultaneously imagine themselves actively performing the represented motion. Prior to actual recording, the process often involves many practice attempts for the subject to learn to elicit neural signals that are *distinct* for each movement and *repeatable* across each attempt. After a sufficient practice period, the clinician guides the subject through a similar training period while active neural signal recording is performed. The recorded data are then used to train predictive machine learning or pattern recognition algorithms. Once trained using signal features from a specific human subject, a pattern recognition algorithm can then be used to predict movement intentions from the subject's neural signals. These predicted movements are converted into real-time control signals for prosthesis activations corresponding to the subject's intent (88).

3.2.2. Problems with Decoding Motor Intent. There are many physiological and engineering constraints that make decoding movement intention from neural signals a challenging, fascinating, and unique application. For one, the brain's complex organization does not lend itself to simple location-based neural recording. It can be presumed that the motor signals driving the limb originate in the primary motor cortex (M1). However, neurons in the premotor cortex and the supplementary motor area also play an active role in encoding motor intentions and actions. Therefore, M1 is typically used as a first choice for movement decoding, especially to help minimize surgical intervention of implanting an electrode array, though it is not uncommon to have MEAs implanted across multiple areas of the brain. Encoded motor information has been obtained from a single MEA in human subjects to demonstrate reach-to-grasp movements (73, 89). However, more complex movements such as planning or dexterous manipulation may not be fully captured by a single MEA. In that case, multiple MEAs can be implanted, and complex decoding has been demonstrated in nonhuman primates (6, 90). Additionally, the full availability of spatially dispersed electrodes coupled with temporal information has enabled the decoding of different motor tasks and movement trajectories (91, 92). LFP signals, in conjunction with the single and multiunit signals, can also provide complementary information that improves decoding performance (93). Further compounding the problem of decoding motor signals, the anatomy of each individual human subject varies substantially, and his/her cortical mapping can change with respect to neurologic injury type leading to highly personalized implant procedures. Therefore, a one-size-fits-all decoding solution remains elusive.

The use of machine learning tools for movement decoding requires an assumption that future incoming neural signal data will resemble the corresponding signals collected during algorithm training. However, many contextual factors conspire to ensure that this assumption is not always valid. Variations in the neural signals over time, the experimental conditions, and the use conditions can all negatively affect decoding performance. For example, when using EMG for hand and finger movement decoding, changes in upper-limb positions (82, 94) or prosthesis loading conditions (95) will affect the supporting muscle contributions and, consequently, alter the recorded muscle-activation signals. Contextual changes in any neural signal modality can significantly degrade movement-decoding performance if those factors are not accounted for during training. This necessity for condition-variant training presents another difficulty at the clinical level: accommodating each condition during training is onerous and quickly becomes burdensome for the user. As a result of extensive, often daily training, prosthesis users may choose to abandon neurally controlled prostheses for simpler, more reliable alternatives such as body-powered prostheses (96).

There are other factors hindering reliable and consistent motor decoding, which likely cannot be accounted for during the training process. Recording electrode conduction properties, for example can change over time. For chronically implanted MEAs, a well-known problem is gliosis, a form of scarring caused by the accumulation of glial cells at the electrode penetration site, which degrades

the recording quality of neural signals over time (76, 77). Considerations must be made for the electrode metals and materials based on their application to achieve the desired recording properties while also minimizing biorejection. Problems such as micromotion, damage to microvessels, and physical changes in the electrode–body interface (e.g., gliosis) cause drifting or corruption of the neural signal feature data, leading to poor decoding performance. At the cognitive level, spontaneous neural activity may also exhibit different patterns for the same output motion. For example, neural signals activated for reaching and grasping of an apple during hunger may not resemble those for reaching and grasping for a door handle. In essence, movements can be similar or synonymous at the muscular activation level, but the cognitive motivation for each may be dissimilar.

The result of these combined factors is that offline performance assessments of current methods may differ from their real-time online performance, and experimental results may not reliably translate to improvements in a prosthesis user's performance of daily living tasks. Reliable motor control is, in many ways, a two-way learning problem: using machine learning tools to decode movement intent from neural signals and the prosthesis user learning through sustained practice how to produce consistent neural patterns for each desired movement.

3.3. State of the Art

Despite drawbacks, there is reason to believe that it is possible to achieve intuitive, adaptive, and reliable neural prosthesis control from the subject's full sensory, motor, and cognitive capabilities. Research in motor prosthesis control has led to the development of advanced dexterous prostheses such as the JHU/APL MPL, which has 17 controllable degrees of freedom and 26 total joints throughout the shoulder, elbow, wrist, and fingers (48). EEG signals have been used to deliver one-dimensional (97, 98) and two-dimensional cursor control (99), as well as enabling the control of wheelchairs (100) and robotic limbs (101). ECoG has been used as a control signal for cursor control in one (102, 103) and two dimensions (104, 105). ECoG has also been used for the operation of upper limb prostheses (50, 64, 70, 106), including individual finger movements (49).

Surgical techniques such as TMR have been devised where nerves from an amputated limb are embedded into alternative healthy muscle material that is no longer attached to the missing limb (79). The reinnervated muscles act as biological amplifiers for the neural motor signal, which can then be used for prosthesis control (107). Post-TMR amputees have shown dramatic improvement in simultaneous and proportional EMG control (108). Furthermore, recent work has shown that TMR patients can achieve robust prosthesis control using high-density EMG signals, which are then decomposed into motor unit spiking information using blind source separation techniques (109). Osseointegration, a surgical method that creates a static link between the prosthesis and the bone at the site of amputation, has been shown to reduce user retraining while improving task completion in real-world conditions (110). Algorithmic techniques have also been developed to mitigate the degradation of performance resulting from real-world and untrained conditional effects (82, 111, 112).

Currently, no single sensor modality captures the full complexity of the motor-decoding problem, nor the feedback interplay between the prosthesis user's neural signals and his/her environment. Therefore, multimodal approaches to neural prosthesis control are being explored wherein a mixture of sensors are used to incorporate *intrinsic* (from the body) and *extrinsic* (environmental) contextual information into the decoding problem. Hybrid systems incorporating multiple neural signals with eye-gaze tracking and movement primitives have been used to achieve more natural reach-to-grasp movements (113). Augmented reality systems are also being used in movement-decoding tasks by complementing the user's unaided vision with visual representations of force feedback (114). The sections that follow provide additional details on how researchers have begun to "close the loop" of the neural control problem by providing vital sensory feedback information to the prosthesis user.

4. SENSORY NEURAL PROSTHESES

The information flow in sensory neural prostheses is the reciprocal to motor neural prostheses. For sensory devices, the external sensor acquires a signal, which is then sent to the processing unit. To provide the information back to the nervous system, the sensor signal is encoded based on the stimulation needed to achieve a functional response at the various levels of neural interfacing (cortex, spinal cord, or peripheral nerves) to elicit the desired target sensation, such as touch, vision, or hearing (Figure 8). Perhaps the best example of a commercially successful neural prosthesis is the cochlear implant. The cochlear implant

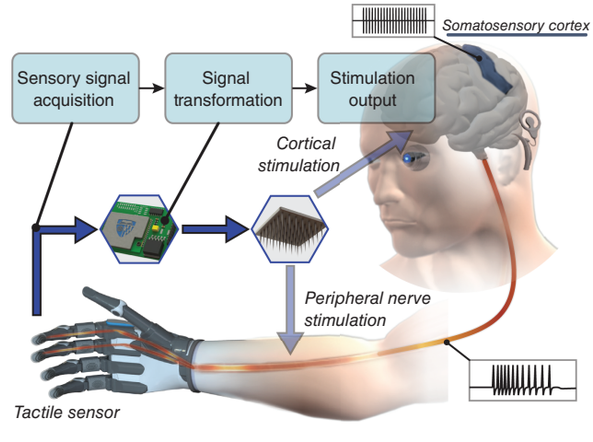

Figure 8. In sensory neural prostheses, some external sensor measurement, such as touch on a prosthetic hand, is recorded and sent to the processing unit. The sensor signal is transformed into unique stimulation patterns to be sent to either the peripheral nerves or the cortex. The stimulation pattern is determined by the neural target for stimulation to elicit a more natural perception.

conveys audio to a hearing-impaired user by directly stimulating the auditory nerve (115, 116). In a similar manner, stimulation of the optic nerve or retinal ganglion cells can provide rudimentary visual feedback. Similar to how the auditory nerve preserves neural pathways even after damage to the inner ear hair cells, degeneration of the retinal light-sensitive rods and cones does not affect signal transmission from the retinal ganglion cells through the visual pathways. Because of this, electrical stimulation of the retina, optic nerve, or visual cortex results in visual percepts in blind subjects (117, 118). Another device whose primary function is sensory feedback is the vestibular neural prosthesis, which aims to restore balance during movement by stimulation of the nerve fibers in the semicircular canal (SSC) (119).

Equally important to the ability to control a motor prosthesis, such as an arm, is the need to have bidirectionality, the ability to receive feedback, such as in the form of touch or proprioception, from the prosthesis. Users of traditional prosthetic limbs (i.e., without sensory feedback) often rely on visual information, especially during grasping or hand movements, to monitor their device. In some cases, experienced myoelectric prosthesis users can use sounds of motors within the prosthesis as audio feedback to determine when or how far the hand has moved; however, this is not always a practical form of sensory feedback. For lower limb prostheses, users typically rely on gross pressure from loading during gait to determine movement and contact. The perception of minute shifts in weight is often lost, resulting in poor balance and symmetry (120).

Neural mechanisms for perceptions of taste (121, 122) or the sense of smell (123, 124) have been investigated, but providing those sensations to users through a neural interface has yet to be thoroughly researched. However, as understanding and technology develops, specifically neural interfaces, devices to restore the sense of smell (125) or taste (126) could become more prevalent. In the following sections, we will highlight several advances in neural interface technology for achieving sensory feedback in neural prostheses via the dominant modality of stimulating the PNS and CNS. Although many hardware developments discussed here are intended for use with upper limb prostheses, the interface and approach for providing feedback between the different senses (i.e., touch, vision, and hearing) are similar. The differences lie in the targeted neural regions and parameters of the stimulation.

4.1. Methods of Sensory Interfacing

To further define some of the fundamental components discussed in previous sections, the primary interfaces for the sensory components of neural prostheses are: (i) the physical sensors themselves, which measure some external physical property such as pressure (for touch) or inertial sensor (for position) and (ii) the stimulating electrodes in either the PNS or CNS, which provide the sensory feedback to the user. This requires innovations in sensors as well as stimulating electrode technologies. Hardware advances and electronic miniaturization have resulted in specialized sensors for sensory feedback, and electrode technologies implemented to miniaturize packages for eventual implantation. As a result, interest in improving the neural interface and understanding the physiological relationships between stimulation and perception for providing high-quality feedback has increased. Important considerations for neural prosthesis sensors are the size of the sensor and electronics as well as the resolution of the signal. For the neural interface on the other hand, the specificity of the electrodes (i.e., how well they can selectively stimulate the target) is of upmost importance to ensure high-quality and naturalistic feedback.

4.1.1. Sensors. The crucial role of sensors is providing useful input to prostheses for restoring sensory impairment. In the case of the cochlear implant, the sensor is an external microphone that captures sound for an onboard speech processor. Wireless transmission to a receiver interprets the decoded speech and translates that signal to the corresponding stimulating electrodes within the cochlea (116, 127) (Figure 9a). For the case of vestibular neural prostheses, three gyroscopes are traditionally used to measure head roll, pitch, and yaw (119) (Figure 9b). Cameras are often used for visual neural prostheses to capture images, and a processor translates that information to the implanted stimulator on the retina or in some cases the optic nerve or visual cortex directly (9).

The most common sensing modalities for upper limb neural prostheses are grip force and pressure. The sense of touch plays a crucial role in basic hand movements and exploratory actions (131, 132). These sensations can be quantified as force or pressure signals from various parts of the hand. The cutaneous neurons found in healthy skin, namely the rapidly and slowly adapting types I and II (RAI, RAII, SAI, and SAII), respond primarily to changes in force (133). For a more in-depth discussion of the types of mechanoreceptors and their physiological behaviors, see (133). Grounded in physiological similarities as well as ease of implementation, force and pressure measurements are the most basic sensing modalities for upper limb neural prostheses; however, they are by no means the only component of tactile sensing. Two current examples of fingertip sensors for upper limb neural prostheses are the BioTac, developed by SynTouch (128) (Figure 9c), and the fingertip sensing nodes (FTSN), developed by the JHU/APL for the MPL (129) (Figure 9d). The sensors can detect a wide range of forces experienced during grasping with a prosthesis. The BioTac has also demonstrated the ability to measure vibrations to discriminate between different textures (134). The FTSN is fully integrated into the MPL for measuring relevant force information. Although the numerous internal sensors on the MPL are used primarily for local feedback (i.e., to the prosthesis), the contact and force signals of the FTSN are the primary inputs to the user for sensory feedback as these contain the most relevant and currently translatable information. Another example of a prosthetic hand force sensor is the flexible, textile piezoresistive finger cuffs developed in Reference 130 (Figure 9e). It should be noted that force and pressure are only subsets of a much more complex set of perceptions that make up the sense of touch. Tactile sensation is made up of additional perceptions such as curvature, torque, slip, friction, texture, and pain. These

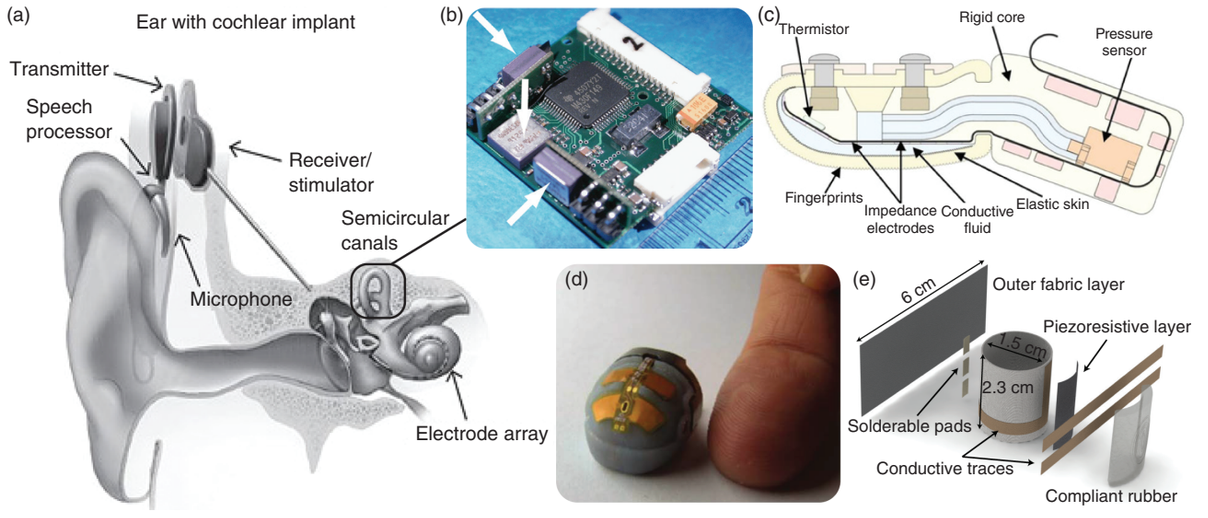

Figure 9. Sensors for neural prostheses. (a) Cochlear implant with external microphone and processor for capturing and interpreting speech. Source: Reprinted, with permission, from (127). (b) Internal gyroscope (white arrows) for a vestibular prosthesis. The output of the gyroscope drives stimulation of the semicircular canals of the vestibular system. Source: © 2007 IEEE. Reprinted, with permission, from (119). (c) The BioTac, developed by SynTouch, uses conductive fluid and changes in impedance to determine pressure. Source: Reprinted from (128) under the CC-BY license. (d) Fingertip sensing node (FTSN) developed by the JHU/APL. The FTSN detects force along three axes using a load cell; it also contains vibration detection through accelerometers, temperature, and contact (129). Source: © 2014 Johns Hopkins University/Applied Physics Laboratory LLC. All Rights Reserved. For permission to use, modify, or reproduce, contact the Office of Technology Transfer at JHU/APL. (e) A textile, piezoresistive tactile sensor for measuring fingertip forces on prosthetic hands. Source: © 2014 IEEE. Reprinted, with permission, from (130).

complex components of touch are hard to capture using traditional fingertip sensors. Additionally, skin dynamics play a major factor in the perception of touch (135) and have been taken into account in one technique that models receptor behavior (136). Current sensors can detect basic components of touch, but are still primitive compared to the sophisticated ability of receptors found in healthy skin.

4.1.2. Neural Sensory Interfaces. For sensory neural prostheses, invasive surgery is often required to implant stimulating electrodes. Two primary concerns for connecting electrodes to the nervous system are biocompatibility and long-term stability. For a more detailed discussion of neural electrodes, including material considerations, see Reference 26. In general, sensory neural prostheses utilize one of the electrode types discussed in Section 2. However, there can be modifications to the stimulating neural interface based on the properties of the targeted system. For instance, a cochlear implant uses an array of platinum contacts embedded within silicone that is inserted into the cochlear duct (Figure 9a). The base and apex of the cochlea respond to the highest pitches of sound (~20 000 Hz) and the lowest pitches (~200 Hz), respectively. The region of the cochlea between the base and the apex corresponds to the range of frequencies between the extremes. As a result, cochlear implant electrodes target different regions between the base and apex to elicit percepts of various sound frequencies. Owing to the proximity of the vestibular apparatus to the cochlea, the same electrode materials and stimulator can be used for a vestibular neural prosthesis as well (Figure 10a). The vestibular system contains three SSCs that respond to angular head rotations. The canals are orthogonal to each other, allowing for stimulation of each SSC for an independent axis of head rotation (119). After implantation, stimulation of each vestibular electrode site creates perception of head movements about a different axis of rotation, which can be quantified by measuring ocular reflex responses based on the perceived head movement (137, 139). In many visual prostheses, an electrode array is placed directly on the retina to bypass damaged photoreceptors (138) (Figure 10b). For a retinal implant, the individual electrodes are 200 μm in diameter with a spacing of slightly over 500 μm (138). In some cases, stimulation of the optic nerve (140) or penetrating microelectrodes in the visual cortex provide feedback (141). The sensory interface to the PNS is similar to the CNS in that penetrating MEAs are often used for stimulating nerve bundles, specifically for sensory feedback in upper limb prostheses (142).

4.2. Feedback

Because of the complex nature of neural pathways and synapses to multiple regions of the brain before an external sensory signal is perceived, it is more advantageous to provide sensory feedback stimulation as close to the biological sensor (i.e., hair cells in the ear, photoreceptors in the eye, or mechanoreceptors in skin) as possible. By stimulating as close to the source of signal transduction (i.e., the biological sensor) as possible, the stimulation signal passes through the same neural pathways as a signal from a healthy biological sensor. It should be noted

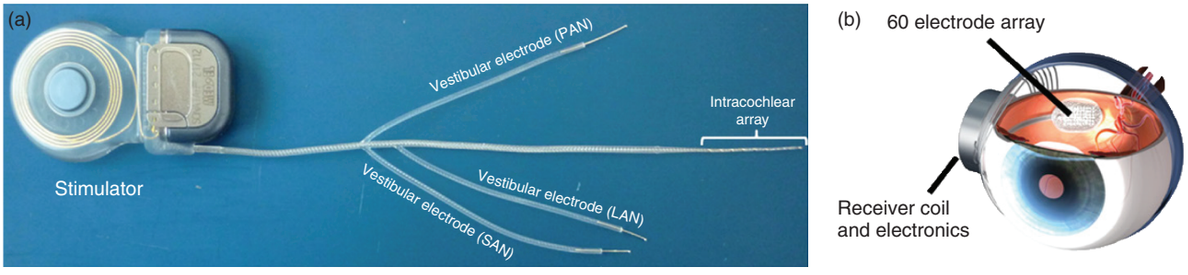

Figure 10. (a) Stimulator with electrodes for a cochlea and vestibular neural prosthesis. A stimulating electrode is used to excite the posterior ampullary nerve (PAN), lateral ampullary nerve (LAN), and superior ampullary nerve (SAN) in the SSC of the vestibular system for helping restore balance. Source: Reprinted from (137) under the CC-BY license. (b) A visual prosthesis electrode array implant that bypasses damaged photoreceptors and stimulates the retina directly. Source: Reprinted from (138) under the CC-BY license.

though that issues of cortical plasticity and remodeling may influence sensory perception. A classic example is cortical reorganization after digit amputation in nonhuman primates (143); however, more recent research has shown that spatial acuity does not increase in humans after digit amputation (144). One thought is that somatotopy is preserved to some extent after long-term deafferentation (145). The idea of preserved somatotopy is supported by recent results showing sensory activation of the phantom hand in multiple amputees through direct peripheral nerve stimulation 16 and 21 years after amputation (146) and transcutaneous stimulation of peripheral nerves in a subject five years after amputation (147). These results suggest that cortical representation of sensory regions remains in some capacity even several years after an amputation; however, the issue of cortical plasticity, particularly in cases of amputation, is an area of ongoing research. The known physiological behaviors of the biological sensors, such as the transducing mechanisms and corresponding output signals, can be leveraged to design more realistic and functional neural prostheses. A good example of this is the cochlear implant. Electrical stimulation of auditory nerve fibers in the cochlea can restore hearing. Loss of hair cells in the cochlea results in inefficient processing of auditory signals, so the cochlear implant directly stimulates the surviving fibers of the auditory nerve as opposed to the auditory cortex because the behavior and tonotopic organization of the cochlea are better understood and easier to access for a neural prosthesis (148, 149).

4.2.1. Cochlear Implants. Cochlear implants work best in users who have fully developed auditory neural pathways but have lost hearing due to damage to the hair cells in their cochlea. The cochlear implant bypasses the damaged cells and directly stimulates the auditory nerve fibers. One problem that arises is that implants cannot be directly inserted all the way into the cochlea. Because of the tonotopic organization of the cochlea, this results in low-frequency regions (apex) not always being stimulated. However, surgical techniques have improved the ability to reach more apical regions (150). To combat this, a compressed analog (CA) strategy was used to separate the sound by frequency and stimulate only electrodes corresponding to that frequency in the cochlea. Because of overlap in the electric fields from adjacent electrodes, research suggests that there are typically only between 4 and 8 independent electrodes even in arrays with as many as 22 electrodes (8). This is a severe limitation of the CA encoding method, which was addressed by the novel continuous interleaved sampling (CIS) strategy. CIS gives brief pulses to stimulating electrodes in nonoverlapping sequences, resulting in much higher levels of speech recognition (151, 152). Understanding of mechanical frequency decomposition within the cochlea and how areas of the brain respond led to the discovery that signal envelope is most important for speech perception, and fine time structure (i.e., frequency) is most important for pitch and localization (153). More recent feedback methods propose to more closely mimic, in a biologically relevant way, how these pieces of auditory signals are transmitted through the auditory nerve (154). Although the ability of users to perceive natural speech and pitch is not perfect and allows for a rather gross representation of sound (155), many users take several years to improve their ability to perceive speech with continued improvement even beyond 8 years after being implanted (156). For a more thorough review of cochlear implants to restore hearing, see Reference 8.

4.2.2. Retinal Prostheses. The primary physiological principles for visual neural prostheses are that (i) light can be replaced by electric current to elicit the perception of vision, (ii) blindness due to retinal degeneration does not affect signal transmission from the retinal ganglion cells through the visual pathways, although remodeling can occur in the retina over time, and (iii) electrical stimulation of the visual pathways and visual cortex can elicit visual percepts in blind subjects (117). It should be noted that for visual impairment from retinal degeneration it is not known what impact any retinal remodeling has on the retinal ganglion cell structure and function, which would potentially affect the visual perceptions generated from direct retinal ganglion cell stimulation. Visual feedback is achieved by stimulating the retina, the optic nerve, or the visual cortex directly. Each method for feedback presents its own benefits and shortcomings, but the most common approach, especially in currently available commercial solutions, is through retinal stimulation (138). Damage to

photoreceptors occurs due to AMD and retinitis pigmentosa (RP), but the photoreceptors can be bypassed with retinal stimulation. The advantage of retinal stimulation in blind subjects with AMD and RP is that neural pathways are still intact, so visual information is processed and perceived in the same manner as before visual degeneration, assuming there are no major changes in cortical mapping of visual information. One of the many drawbacks to retinal implants is the limited space to place the electronics on the retina. Other important factors include size of the electrode as well as stimulation charge density and resolution. Stimulating a small area of the optic nerve using a cuff electrode presumably activates a larger portion of the visual field due to the increased density of target axons within the nerve compared to the retina. The downside is that detailed perception and stimulation specificity are difficult to achieve. In addition, optic nerve stimulation is not as well researched compared to retinal stimulation (157). Finally, visual cortex stimulation is possible and has been used historically for visual feedback (141) but requires a brain surgery, with accompanying high risk, and technology to implant the stimulator in the brain that add to the complexity of the system. For a more thorough review of restoring vision through a neural prosthesis, see References 117, 157. For a discussion of biological challenges, see Reference 158.

4.2.3. Upper Limb Prostheses. Recently, sensory feedback for neural prostheses has been used to restore the sensation of touch to upper limb amputees or individuals with SCI. Restoring sensations of touch through cortical stimulation has been achieved in healthy nonhuman primates (53) as well as humans with SCI (52) and paralysis due to nerve injury (159). Stimulation to provide tactile sensation can be applied at the cortical (52, 53) or peripheral (10, 142, 160) levels. Perceptions of touch can be achieved through a cortical neural interface by targeting neurons in the S1. The somatotopic organization for tactile representation in S1 enables researchers and surgeons to target specific regions that correspond to activation of tactile sensation in the hand, or the phantom hand in the case of an amputee. The quality and type of tactile perception is of great interest to ensure a more natural and intuitive neural prosthesis. It was shown that nonhuman primates can discriminate between different intracortical microstimulations (ICMS) and localize the sensation between different fingers almost as well as if their actual fingers were touched (53). Developing neural prostheses through human research volunteers provides an additional advantage in that more detailed data on perception and usability can be acquired. Specifically, the type of tactile perception can be recorded based on user feedback. With 60 penetrating microelectrodes in S1, stimulations of tens of microamperes are enough to provide the sense of touch in multiple distinct regions of the hand (52) (Figure 11a). Those perceptions are described as touch, pressure, vibration, electrical tingling, and even temperature in some cases. The stimulation in S1 is perceived by the user as being "possibly natural," which falls in the middle of being "totally natural" or "totally unnatural" (52).

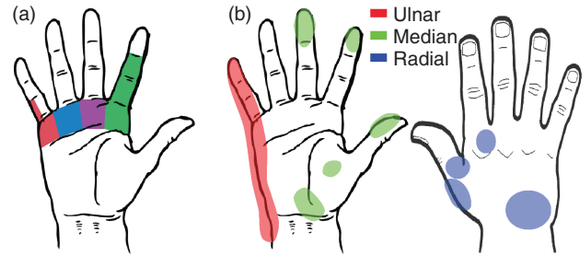

Figure 11. Areas of phantom hand activation from neural stimulation for touch feedback in human amputee subjects. (a) Cortical stimulation using multiple penetrating MEAs in S1 can elicit sensations in unique areas of different fingers. Source: Results adapted from (52). (b) Peripheral nerve stimulation using cuff electrodes on the ulnar, median, and radial nerves of an amputee elicits tactile sensations. Source: Results adapted from (10). In both the cases, stimulating targeted sensory neurons elicits perceptions of tactile activation in the hand/phantom hand.

One drawback to cortical stimulation for touch feedback is the relatively high-risk surgery involved with implanting electrodes. An alternative is implanting electrodes in peripheral nerve afferents, which carry sensory information back to the CNS. The benefit to this approach is the less traumatic surgery to implant the nerve-stimulating electrodes. Even through peripheral nerve stimulation, sensations in regions of the phantom hand, in the case of amputees, are still activated (10, 146) (Figure 11b). In addition, the site of stimulation is closer to where the biological sensors (i.e., the mechanoreceptors in the skin) once were. As already mentioned, this allows the stimulation feedback signal to pass through existing neural pathways, which potentially allows for more naturalistic processing by the nervous system. However, this method does not work for individuals with spinal cord injuries that prevent neural signals from traveling from the periphery to the cortex. Another issue is the lack of somatotopy within nerve bundles. Major nerve bundles (i.e., median, ulnar, and radial) are very well understood in their innervation in the hand and forearm. The problem is that within each nerve bundle, the individual nerve fibers, both afferent (i.e., sensory) and efferent (i.e., motor) nerve fibers, are intermingled with no apparent separation. To combat this issue, surgeons can differentiate between afferent and efferent fibers by stimulating to see if a muscle contracts, indicating an efferent fiber. If the subject is awake during the implantation, then stimulation of afferent fibers and the perceived location and sensation can be mapped by the subject to guide the site for final electrode implantation. Cortical stimulation (52, 159) appears to activate larger regions and fewer distinct locations of perceived activation in the hand compared to some reports of peripheral nerve stimulation (10, 142) for touch feedback given the number of stimulating electrodes. This could be due to the larger density of sensory neurons in the cortex compared to the peripheral nerves. While it is possible to get distinct activation in different fingers using stimulation at either level, it seems more likely to get better specificity (i.e., smaller regions of activation) through peripheral nerve stimulation for touch feedback.

Several upper limb amputees with implanted peripheral nerve electrodes have shown the ability to incorporate touch feedback for discriminating between objects (160) and improved ability with handling delicate objects (10). Peripheral nerve activation for touch feedback can also be achieved using transcutaneous electrical nerve stimulation (TENS), which uses an electrode to activate the nerve through the skin. This method requires no electrode implantation or surgery and has been shown to restore the sense of touch in upper limb amputees (147, 161); however, the downside is the lack of specificity of stimulation within the nerve bundle. The afferents connected to mechanoreceptors in healthy skin have similar physical size so it is difficult to activate a fiber population of a specific mechanoreceptor type, such as rapidly adapting (RA) or slowly adapting (SA). By making peripheral nerve stimulation pulses constant in intensity, a mixed population of fibers are activated in synchrony, which gives rise to the "tingling" from electrical stimulation (10). Finding the correct stimulation patterns in human subjects to minimize the unnatural perceptions and elucidate more realistic sensations of touch and pressure is an ongoing area of research with promising results (162).

Another approach for providing tactile feedback is through mechanical stimulation of receptors in the skin. Research has shown the ability to provide mechanical stimulation of amputee's forearms to provide feedback from the prosthesis fingertips (163) and to aid in prosthesis embodiment (164). These methods are a form of sensory substitution where one mechanism, such as the sense of touch, is mapped to another modality or location, such as mechanical stimulation of the forearm. Research has also shown that transcutaneous mechanical stimulation of peripheral nerves can elicit natural tactile sensations in an amputee (30), which suggests that electrical stimulation is not the only way to provide natural sensory feedback in a neural prosthesis.

In any case, quantifying how different stimulation patterns and amplitudes influence perception of sensory feedback is important for better understanding of how users will be able to incorporate and utilize the neural prosthesis. Because neural stimulation for tactile feedback is still a relatively new area of research, the most significant studies over the past several years have involved psychophysics and fundamental experiments to evaluate how the stimulation is being perceived by the user (10, 52, 142, 159, 160, 162).

4.3. State of the Art

While most attempts at restoring sensory perception focus on vision, hearing, and touch, restoring the sense of smell (olfaction) through neural stimulation has seen recent developments. Stimulation to provide smell would likely occur in the CNS in the olfactory bulb or olfactory nerve (124, 165), both of which are located on the inferior and rostral region of the brain, or even the olfactory cortex. Although this work is still in its infancy, the idea for a neural prosthesis to restore olfaction has been patented (125). Taste restoration is also a sensation that will undoubtedly be investigated in the future (126) although current tongue prostheses primarily focus on movement (i.e., swallowing) instead of restoring the perception of taste (166). To restore the sense of taste, stimulation could occur in the CNS through the gustatory cortex or the relevant facial nerve branches.

The most recent developments in sensory neural prostheses are in restoring balance through vestibular stimulation (167) and restoring the sense of touch through cortical (52) or peripheral nerve stimulation (10, 142, 160). The possibility of a neural prosthesis that restores an entire limb, using both forward motor control and sensory feedback, has spurred several significant discoveries and technologies. One novel surgical technique for increasing the ability to provide sensory feedback through peripheral nerve stimulation is targeted sensory reinnervation (TSR). In TSR, the surgeon separates sensory fibers from the median, ulnar, and radial nerves, which then innervate in tissue and skin, making it easier to target specific regions of an amputee's phantom hand for tactile feedback (30). This technique is like TMR, which enables more intuitive motor control of a prosthetic limb, in that nerve fibers are directed to predetermined locations; however, the difference is that in TMR motor (efferent) nerve fibers innervate large muscle to amplify and separate motor signals. In TSR, sensory nerves (afferents) are placed such that they innervate tissue in a structured manner, which makes it easier to identify regions of stimulation for sensory feedback.

Neural interfaces and systems for upper limb devices are not at the same level of commercial prominence as cochlear or retinal implants, but as the technology for bidirectional prosthetic limbs continues to improve there will likely be a growth in commercial viability and interest. Part of the uncertainty for upper limb neural prostheses is in the long-term functionality and benefit of the devices. Research has already shown the benefit of incorporating touch feedback into prosthetic limbs for improving grasping functionality (168) as well as in-depth studies on sensory perceptions of stimulation (162). Recently, researchers induced a kinesthetic illusion in amputee subjects to provide the sensation of movement and improve both prosthesis control and embodiment (169). In addition to understanding the user's perception of tactile and positional feedback, it is important to improve the perception of the prosthetic hand itself to the environment through sensory feedback. This includes developing reflex-like algorithms that utilize tactile feedback for preventing accidental object destruction or slip through improper grasping. While grasping functionality is improved through tactile feedback to the user (10, 168), there is also improved grasping functionality when tactile feedback to the prosthesis triggers intelligent, programmed automatic responses of the artificial system to act like a reflex to prevent object damage or slip during grasping (170). The combination of sensory feedback to both the prosthesis and the user is crucial for creating a realistic and intelligent neural prosthesis.

Another approach for enhancing neural prostheses for touch feedback is using biomimetic stimulation patterns. In theory, applying stimulation that matches actual neuron behavior, whether from neurons in S1 or

mechanoreceptors in the PNS, would create more realistic sensory perceptions. The technological limitation though is in the hardware and surgical inability to reliably target specific populations of neurons, such as RA or SA afferents. Research groups have already developed sophisticated and realistic models that closely mimic real neural behavior using bifurcation methods to reduce classical Hodgkin–Huxley-type models to more computationally efficient ones (171) or simple models of mechanotransduction (172). Recently, mechanoreceptor-specific models from physiological data have been developed for SA and RA afferents covering the whole hand (136). Modeling the neural behavior at the receptor level theoretically enables one to reproduce complex types of tactile perceptions if peripheral nerve afferents could be reliably identified and stimulated. An emerging technique, called neuromorphic engineering, is based on the idea of mimicking neurobiological architecture found in the nervous system. Here, the sensor (or receptor) output is encoded in the form of spiking neural activity, and then subsequent processing is used to provide relevant sensory information back to the prosthesis user. In recent examples of this approach, a neuromorphic tactile signal can be used by a prosthesis to control grip force during grasping (173), and a neuromorphic stimulation model was shown to allow an upper limb amputee to discriminate between textures being applied to a prosthetic finger (174).

Current state-of-the-art limbs such as the MPL include force sensors, which have been sufficient for understanding basic perceptions such as grasping objects and preventing slip; however, current fingertip sensors are inadequate to capture the more intricate subtleties of touch. Benefits of providing more advanced tactile feedback to users, such as shape and even temperature or pain, will require further research both in feedback methods and sensor technology. As stimulation methods and neuron models become more advanced, there inevitably will be the need for more sophisticated and realistic sensors to produce biomimetic signals. One recent example is a skin-inspired digital mechanoreceptor that produces spiking activity during loading (175). The digital mechanoreceptor behaves similarly to an actual mechanoreceptor in the skin and could be placed directly on a prosthetic hand as a synthetic skin. Another approach is a biologically inspired multilayered tactile sensor that is structured to give varying responses from the different layers based on applied loads (176), similar to how different mechanoreceptors respond differently to the same inputs (133). To be even more realistic, some synthetic skins have even shown the ability to self-heal (177, 178), which could also be used as a smart electronic skin (e-skin) for a prosthetic hand. A more detailed review of e-skins can be found in Reference 179. The parallel development of neural interfaces, sensors, and stimulation methods will lead to more enhanced ways for providing naturalistic tactile feedback to upper limb prosthesis users.

5. FUTURE DIRECTIONS

The track record of success for cochlear implants and visual prostheses offers strong evidence in support of the continual progress being made in neural prostheses and neuroengineering in general. Several challenges remain for improving upper limb prosthesis control. On the signal recording side, one example is improving resolution of ECoG. In employing MEAs or other neural recording techniques there is a need for providing better localization to areas of the cortex responsible for dexterous hand and finger movements. Another area of continued improvement is the development of decoding algorithms that are designed specifically to handle neural signals from large arrays of electrodes. The recent interest in upper limb prostheses presents a unique challenge because the system is bidirectional, requiring both forward motor control as well as sensory feedback. This bidirectional requirement is an engineering challenge because it relies on a neural interface for capturing motor intent as well as a neural interface for providing sensory feedback. It also requires the combination of sophisticated decoding algorithms for limb movement as well as techniques for encoding and conveying sensory information to the user. The perception of touch is just the beginning for incorporating sensory information in prosthetic arms. Additional sensory perceptions such as proprioception, temperature, and pain would be desirable for creating a truly biomimetic prosthetic limb. The technology is in place to show how something as complex as an arm can have be controlled with neural motor signals while also providing sensory feedback to the user. A major hurdle to having a functional neuroprosthesis, with either motor or sensory (or both) interfaces, is the long-term stability of these systems, especially ones that utilize cortical neural interfaces. Research is expected and encouraged to investigate the efficacy of prosthetic limbs for both amputees and individuals with spinal cord or nerve injury through clinical trials focusing on rehabilitation and functionality assessments. Finally, there are many ethical considerations with neural prostheses because the selection of subjects to be implanted with a long-term device must be evaluated in terms of potential risks and benefits for each individual.

One possibility for future neural prostheses is the fusion of multiple sensing modalities for improved performance. An example of this is combining visual and tactile sensor information to enhance the ability of a robotic arm to move through space and manipulate objects, making it more lifelike and intuitive to control. Other future trends may include the use of augmented reality to provide relevant information about a neural prosthesis back to the user or even the potential for creating real-world training scenarios for motor prostheses, specifically prosthetic arms.

Although upper limb neural prostheses are currently in the limelight, the same technological advancements in motor control and sensory feedback can be applied to lower limb prostheses as well as exoskeletons. The sense of touch is not as crucial for a lower limb prosthesis, but as the technology matures there will undoubtedly be efforts to restore the sensation of contact at different parts of the foot during walking, which will likely have a benefit on user's performance and functionality. Other senses, namely taste and smell, are yet to be researched as thoroughly as the sense of

touch or the ability to move a limb with your thoughts, but they are still valid systems for neural prostheses. The ability for any neural prosthesis to completely and perfectly replace a lost function still alludes the scientific community, but the ever-increasing rate of innovation will continue to bring us closer.

ACKNOWLEDGMENTS

Images reproduced from open access sources are done so under the Creative Commons Attribution 3.0 license.

LIST OF TERMS

Afferent	The nerve fiber of a sensory neuron
Axon	A nerve fiber
Biomimetic	Of or relating to synthetic methods that mimic a biological process
Efferent	The nerve fiber of a motor neuron
Gliosis	CNS response to acute injury
Mechanoreceptor	A sensory receptor found that responds to mechanical changes
Neuroprosthesis	A colloquial term used for a neural prosthesis
Neuroprosthetics	A field of study relating to development of neural prostheses
P300	Event-related potential component associated with decision-making
Prosthesis	(noun) An artificial body part or organ (plural prostheses)
Prosthetic	(adjective) Of or relating to a prosthesis

LIST OF ABBREVIATIONS

ADC	analog-to-digital converter
AMD	age-related macular degeneration
BCI/BMI	brain–computer/machine interface
CA	compressed analog
CIS	continuous interleaved sampling
CNS	central nervous system
ECoG	electrocorticography
EEG	electroencephalography
EMG	electromyography
ERD/ERS	event-related de/synchronization
FINE	flat interface nerve electrode
FTSN	fingertip sensing node
HD-USEA	high-density Utah slanted electrode array
ICMS	intracortical microstimulations
JHU/APL	Johns Hopkins University Applied Physics Laboratory
LAN	lateral ampullary nerve
LFP	local field potential
LIFE	longitudinally implanted intrafascicular electrode
M1	primary motor cortex
MEA	microelectrode array
MPL	modular prosthetic limb
NRIC	near-field resonant inductive coupling
PAN	posterior ampullary nerve
PNS	peripheral nervous system
RA	rapidly adapting
RP	retinitis pigmentosa
S1	primary somatosensory cortex
SA	slowly adapting
SAN	superior ampullary nerve
SCI	spinal cord injury
SSC	semicircular canals
SSVEP	steady-state visually evoked potentials
TENS	transcutaneous electrical nerve stimulation
TIME	transverse intrafascicular multichannel electrode
TMR	targeted muscle reinnervation
TSR	targeted sensory reinnervation
VLSI	very-large-scale integration

RELATED ARTICLES

Biomedical Engineering; Biomedical Sensors; Electroencephalography; Electromyography; Medical Signal Processing; Microelectrodes; Neurotechnology; Retinal Prosthesis; Surface Electromyography (sEMG); Tactile Sensors; Artificial Limbs.

BIBLIOGRAPHY

1. K. Ziegler-Graham, E. J. MacKenzie, P. L. Ephraim, T. G. Travison, and R. Brookmeyer. *Arch. Phys. Med. Rehabil.* **2008**, *89*(3), pp 422–429. doi: 10.1016/j.apmr.2007.11.005.
2. B. S. Armour, E. A. Courtney-Long, M. H. Fox, H. Fredine, and A. Cahill. *Am. J. Public Health* **2016**, *106*(10), pp 1855–1857. doi: 10.2105/AJPH.2016.303270.
3. B. S. Wilson, D. L. Tucci, M. H. Merson, and G. M. O'Donoghue. *Lancet* **2017**, *390*(10111), pp 2503–2515. doi: 10.1016/S0140-6736(17)31073-5.
4. National Eye Institute and National Institutes of Health. Age-related macular degeneration (AMD). Available at https://nei.nih.gov/eyedata/amd, October 20, 2017.
5. S. Acharya, M. S. Fifer, H. L. Benz, N. E. Crone, and N. V. Thakor. *J. Neural Eng.* **2010**, *7*(4), p 046002. doi: 10.1088/1741-2560/7/4/046002.
6. V. Aggarwal, S. Acharya, F. Tenore, H. C. Shin, R. Etienne-Cummings, M. H. Schieber, and N. V. Thakor. *IEEE Trans. Neural Syst. Rehabil. Eng.* **2008**, *16*(1), pp 3–14. doi: 10.1109/TNSRE.2007.916289.
7. F. V. G. Tenore, A. Ramos, A. Fahmy, S. Acharya, R. Etienne-Cummings, and N. V. Thakor. *IEEE Trans. Biomed. Eng.* **2009**, *56*(5), pp 1427–1434. doi: 10.1109/TBME.2008.2005485.
8. B. S. Wilson and M. F. Dorman. *J. Rehabil. Res. Dev.* **2008**, *45*(5), pp 695–730.
9. J. D. Weiland and M. S. Humayun. *Proc. IEEE* **2008**, *96*(7), pp 1076–1084. doi: 10.1109/JPROC.2008.922589.
10. D. W. Tan, M. A. Schiefer, M. W. Keith, J. R. Anderson, J. Tyler, and D. J. Tyler. *Sci. Transl. Med.* **2014**, *6*(257), p 257ra138. doi: 10.1126/scitranslmed.3008669.

11. A. Prasad and M. Sahin. *J. Neuroeng. Rehabil.* **2012**, *9*(1), p 41. doi: 10.1186/1743-0003-9-41.
12. J. B. Zimmermann, K. Seki, and A. Jackson. *J. Neural Eng.* **2011**, *8*(5), p 054001. doi: 10.1088/1741-2560/8/5/054001.
13. A. Jackson and J. B. Zimmermann. *Nat. Rev. Neurol.* **2012**, *8*(12), pp 690–699. doi: 10.1038/nrneurol.2012.219.
14. H. A. C. Wark, R. Sharma, K. S. Mathews, E. Fernandez, J. Yoo, B. Christensen, P. Tresco, L. Rieth, F. Solzbacher, R. A. Normann, and P. Tathireddy. *J. Neural Eng.* **2013**, *10*(4), p 045003.
15. A. Cukiert, A. Sousa, E. Machado, J. A. Buratini, J. Vieira, V. Ferreira, C. Forster, M. Argentoni, and L. Frayman. *Arq. Neuropsiquiatr.* **2000**, *58*(3A), pp 630–636. doi: 10.1590/S0004-282X2000000400006.
16. T. Boretius, J. Badia, A. Pascual-Font, M. Schuettler, X. Navarro, K. Yoshida, and T. Stieglitz. *Biosens. Bioelectron.* **2010**, *26*(1), pp 62–69. doi: 10.1016/j.bios.2010.05.010.
17. Z. Xiang, S. Yen, S. Sheshadri, J. Wang, S. Lee, Y. Liu, L. Liao, N. V. Thakor, and C. Lee. *Adv. Mater.* **2016**, *28*(22), pp 4472–4479. doi: 10.1002/adma.201503423.
18. C. A. Ayers, L. E. Fisher, R. A. Gaunt, and D. J. Weber. *J. Neurophysiol.* **2016**, *116*(1), pp 51–60. doi: 10.1152/jn.00961.2015.
19. X. Zheng, J. Zhang, T. Chen, and Z. Chen. *Microsurgery* **2003**, *23*(3), pp 268–273. doi: 10.1002/micr.10116.
20. D. J. Tyler and D. M. Durand. *IEEE Trans. Neural Syst. Rehabil. Eng.* **2002**, *10*(4), pp 294–303. doi: 10.1109/TNSRE.2002.806840.
21. S. Lee, S. Sheshadri, Z. Xiang, I. Delgado-Martinez, N. Xue, T. Sun, N. V. Thakor, S. Yen, and C. Lee. *Sens. Actuators B Chem.* **2017**, *242*, pp 1165–1170. doi: 10.1016/j.snb.2016.09.127.
22. G. A. McCallum, X. Sui, C. Qiu, J. Marmerstein, Y. Zheng, T. E. Eggers, C. Hu, L. Dai, and D. M. Durand. *Sci. Rep.* **2017**, *7*, p 11723. doi: 10.1038/s41598-017-10639-w.
23. P. Fattahi, G. Yang, G. Kim, and M. R. Abidian. *Adv. Mater.* **2014**, *26*(12), pp 1846–1885. doi: 10.1002/adma.201304496.
24. T. D. Y. Kozai, N. B. Langhals, P. R. Patel, X. Deng, H. Zhang, K. L. Smith, J. Lahann, N. A. Kotov, and D. R. Kipke. *Nat. Mater.* **2012**, *11*, pp 1065–1073. doi: 10.1038/nmat3468.
25. J. Viventi, D. Kim, L. Vigeland, E. S. Frechette, J. A. Blanco, Y. Kim, A. E. Avrin, V. R. Tiruvadi, S. Hwang, A. C. Vanleer, D. F. Wulsin, K. Davis, C. E. Gelber, L. Palmer, J. V. D. Spiegel, J. Wu, J. Xiao, Y. Huang, D. Contreras, J. A. Rogers, and B. Litt. *Nat. Neurosci.* **2011**, *14*, pp 1599–1605. doi: 10.1038/nn.2973.
26. S. Cogan. *Annu. Rev. Biomed. Eng.* **2008**, *10*, pp 275–309. doi: 10.1146/annurev.bioeng.10.061807.160518.
27. A. Patil and N. Thakor. *Med. Biol. Eng. Comput.* **2016**, *54*(1), pp 23–44. doi: 10.1007/s11517-015-1430-4.
28. S. Nag and N. Thakor. *Med. Biol. Eng. Comput.* **2016**, *54*(1), pp 63–76. doi: 10.1007/s11517-015-1442-0.
29. D. R. Merrill, M. Bikson, and J. G. R. Jefferys. *J. Neurosci. Methods* **2005**, *141*(2), pp 171–198. doi: 10.1016/j.jneumeth.2004.10.020.
30. T. A. Kuiken, P. D. Marasco, B. A. Lock, R. N. Harden, and J. P. A. Dewald. *Proc. Natl. Acad. Sci. U. S. A.* **2007**, *104*(50), pp 20061–20066.
31. J. M. Cayce, R. M. Friedman, E. D. Jansen, A. Mahavaden-Jansen, and A. W. Roe. *NeuroImage* **2011**, *57*(1), pp 155–166. doi: 10.1016/j.neuroimage.2011.03.084.
32. T. May, I. Ozden, B. Brush, D. Borton, F. Wagner, N. Agha, D. L. Sheinberg, and A. V. Nurmikko. *PLoS One* **2014**, *9*(12), p e114529. doi: 10.1371/journal.pone.0114529.
33. B. E. Maimon, A. N. Zorzos, R. Bendell, A. Harding, M. Fahmi, S. Srinivasan, and H. M. Herr. *J. Neural Eng.* **2017**, *14*(3), p 034002. doi: 10.1088/1741-2552/aa5e20.
34. I. Diester, M. T. Kaufman, M. Mogri, R. Pashaie, W. Goo, O. Yizhar, C. Ramakrishnan, K. Deisseroth, and K. V. Shenoy. *Nat. Neurosci.* **2011**, *14*(3), pp 387–397. doi: 10.1038/nn.2749.
35. A. C. Thompson, E. D. Jansen, and P. R. Stoddart. *Curr. Mol. Imaging* **2014**, *3*(2), pp 162–177. doi: 10.2174/2211555203666141117220611.
36. N. V. Thakor. *Sci. Transl. Med.* **2013**, *5*(210), p 210ps17. doi: 10.1126/scitranslmed.3007303.
37. J. Webster. *Medical Instrumentation: Application and Design*, 4th ed.; Wiley: Hoboken, New Jersey, USA, 2009.
38. K. Ng, E. Greenwald, Y. P. Xu, and N. Thakor. *Med. Biol. Eng. Comput.* **2016**, *54*(1), pp 45–62. doi: 10.1007/s11517-015-1431-3.
39. D. A. Borton, M. Yin, J. Aceros, and A. Nurmikko. *J. Neural Eng.* **2013**, *10*(2), p 026010. doi: 10.1088/1741-2560/10/2/026010.
40. R. Jegadeesan, K. Agarwal, Y. X. Guo, S. C. Yen, and N. V. Thakor. *IEEE Trans. Microw. Theory Techn.* **2017**, *65*(1), pp 280–292. doi: 10.1109/TMTT.2016.2615623.
41. S. Ozeri and D. Shmilovitz. *Ultrasonics* **2010**, *50*(6), pp 556–566. doi: 10.1016/j.ultras.2009.11.004.
42. J. S. Ho, A. J. Yeh, E. Neofytou, S. Kim, Y. Tanabe, B. Patlolla, R. E. Beygui, and A. S. Y. Poon. *Proc. Natl. Acad. Sci. U. S. A.* **2014**, *111*(22), pp 7974–7979. doi: 10.1073/pnas.1403002111.
43. C. Liu, Y.-X. Guo, H. Sun, and S. Xiao. *IEEE Trans. Antennas Propag.* **2014**, *62*(11), pp 5798–5806. doi: 10.1109/TAP.2014.2352363.
44. K. Agarwal, R. Jegadeesan, Y. Guo, and N. V. Thakor. *IEEE Rev. Biomed. Eng.* **2017**. doi: 10.1109/RBME.2017.2683520.
45. M. S. Chae, Z. Yang, M. R. Yuce, L. Hoang, and W. Liu. *IEEE Trans. Neural Syst. Rehabil. Eng.* **2009**, *17*(4), pp 312–321. doi: 10.1109/TNSRE.2009.2021607.
46. E. Greenwald, C. Maier, Q. Wang, R. Beaulieu, R. Etienne-Cummings, G. Cauwenberghs, and N. Thakor. *IEEE Trans. Biomed. Circuits Syst.* **2017**, *11*(2), pp 324–335. doi: 10.1109/TBCAS.2016.2609854.
47. E. Greenwald, M. Masters, and N. Thakor. *Med. Biol. Eng. Comput.* **2016**, *54*(1), pp 1–17. doi: 10.1007/s11517-015-1429-x.
48. M. Johannes, J. Bigelow, J. Burck, S. Harshbarger, M. Kozlowski, and T. Van Doren. *JHU APL Tech. Digest* **2011**, *30*(3), pp 207–216.
49. G. Hotson, D. P. McMullen, M. S. Fifer, M. S. Johannes, K. D. Katyal, M. P. Para, R. Armiger, W. S. Anderson, N. V. Thakor, and B. A. Wester. *J. Neural Eng.* **2016**, *13*(2), p 026017. doi: 10.1088/1741-2560/13/2/026017.
50. M. S. Fifer, G. Hotson, B. A. Wester, D. P. McMullen, Y. Wang, M. S. Johannes, K. D. Katyal, J. B. Helder, M. P. Para, R. J. Vogelstein, W. S. Anderson, N. V. Thakor, and N. E. Crone. *IEEE Trans. Neural Syst. Rehabil. Eng.* **2014**, *22*(3), pp 695–705. doi: 10.1109/TNSRE.2013.2286955.
51. J. Collinger, B. Wodlinger, J. Downey, W. Wang, E. Tyler-Kabara, D. Weber, A. McMorland, M. Velliste, M. Boninger, and A. Schwartz. *Lancet* **2012**, *381*(8), pp 61816–61819. doi: 10.1016/S0140-6736(12)61816-9.

52. S. N. Flesher, J. L. Collinger, S. T. Foldes, J. M. Weiss, J. E. Downey, E. C. Tyler-Kabara, S. J. Bensmaia, A. B. Schwartz, M. L. Boninger, and R. A. Gaunt. *Sci. Transl. Med.* **2016**, *8*(361), p 361ra141. doi: 10.1126/scitranslmed.aaf8083.
53. G. A. Tabot, J. F. Dammann, J. A. Berg, F. V. Tenore, J. L. Boback, R. J. Vogelstein, and S. J. Bensmaia. *Proc. Natl. Acad. Sci. U. S. A.* **2013**, *110*(45), pp 18279–18284. doi: 10.1073/pnas.1221113110.
54. V. B. Mountcastle. *J. Neurophysiol.* **1957**, *20*(4), pp 408–434. doi: 10.1152/jn.1957.20.4.408.
55. S. Udin and J. Fawcett. *Annu. Rev. Neurosci.* **1988**, *11*(1), pp 289–327. doi: 10.1146/annurev.ne.11.030188.001445.
56. M. F. Glasser, T. S. Coalson, E. C. Robinson, C. D. Hacker, J. Harwell, E. Yacoub, K. Ugurbil, J. Andersson, C. F. Beckmann, M. Jenkinson, S. M. Smith, and D. C. V. Essen. *Nature* **2016**, *536*(7615), pp 171–178. doi: 10.1038/nature18933.
57. R. Ortner, B. Z. Allison, G. Korisek, H. Gaggl, and G. Pfurtscheller. *IEEE Trans. Neural Syst. Rehabil. Eng.* **2011**, *19*(1), pp 1–5. doi: 10.1109/TNSRE.2010.2076364.
58. C. Guan, M. Thulasidas, and J. Wu. High Performance P300 Speller for Brain–Computer Interface, in *Conf. Proc IEEE Biomed. Circuits Syst. (BioCAS)*, 2004; pp 13–16. doi: 10.1109/BIOCAS.2004.1454155.
59. T. J. Bradberry, R. J. Gentili, and J. L. Contreras-Vidal. *J. Neurosci.* **2010**, *30*(9), pp 3432–3437. doi: 10.1523/JNEUROSCI.6107-09.2010.
60. G. Pfurtscheller and R. Cooper. *Electroencephalogr. Clin. Neurophysiol.* **1975**, *38*(1), pp 93–96. doi: 10.1016/0013-4694(75)90215-1.
61. D. J. McFarland, L. M. McCane, S. V. David, and J. R. Wolpaw. *Electroencephalogr. Clin. Neurophysiol.* **1997**, *103*(3), pp 386–394. doi: 10.1016/S0013-4694(97)00022-2.
62. M. S. Fifer, M. Mollazadeh, S. Acharya, N. V. Thakor, and N. E. Crone. Asynchronous Decoding of Grasp Aperture from Human ECoG During a Reach-to-Grasp Task, in *Conf. Proc. IEEE Eng. Med. Biol. Soc. (EMBS)*, 2011; pp 4584–4587. doi: 10.1109/IEMBS.2011.6091135.
63. T. Pistohl, T. Ball, A. Schulze-Bonhage, A. Aertsen, and C. Mehring. *J. Neurosci. Methods* **2008**, *167*(1), pp 105–114. doi: 10.1016/j.jneumeth.2007.10.001.
64. C. A. Chestek, V. Gilja, C. H. Blabe, B. L. Foster, K. V. Shenoy, J. Parvizi, and J. M. Henderson. *J. Neural Eng.* **2013**, *10*(2), p 026002. doi: 10.1088/1741-2560/10/2/026002.
65. G. Schalk, J. Kubánek, K. J. Miller, N. R. Anderson, E. C. Leuthardt, J. G. Ojemann, D. Limbrick, D. Moran, L. A. Gerhardt, and J. R. Wolpaw. *J. Neural Eng.* **2007**, *4*(3), pp 264–275. doi: 10.1088/1741-2560/4/3/012.
66. N. E. Crone, D. L. Miglioretti, B. Gordon, J. M. Sieracki, M. T. Wilson, S. Uematsu, and R. P. Lesser. *Brain* **1998**, *121*(12), pp 2271–2299. doi: 10.1093/brain/121.12.2271.
67. S. Ray, N. Crone, E. Niebur, P. Franaszczuk, and S. Hsiao. *J. Neruosci.* **2008**, *28*(45), pp 11526–11536. doi: 10.1523/JNEUROSCI.2848-08.2008.
68. N. E. Crone, D. L. Miglioretti, B. Gordon, and R. P. Lesser. *Brain* **1998**, *121*(12), pp 2301–2315. doi: 10.1093/brain/121.12.2301.
69. T. Yanagisawa, M. Hirata, Y. Saitoh, T. Goto, H. Kishima, R. Fukuma, H. Yokoi, Y. Kamitani, and T. Yoshimine. *J. Neurosurg.* **2011**, *114*(6), pp 1715–1722. doi: 10.3171/2011.1.JNS101421.
70. D. T. Bundy, M. Pahwa, N. Szrama, and E. C. Leuthardt. *J. Neural Eng.* **2016**, *13*(2), p 026021. doi: 10.1088/1741-2560/13/2/026021.
71. R. S. Markowitz, J. K. Chapin, M. A. L. Nicolelis, and K. A. Moxon. *Nat. Neurosci.* **1999**, *2*(7), pp 664–670. doi: 10.1038/10223.
72. M. Velliste, S. Perel, M. C. Spalding, A. S. Whitford, and A. B. Schwartz. *Nature* **2008**, *453*(7198), pp 1098–1101. doi: 10.1038/nature06996.
73. L. R. Hochber, D. Bacher, B. Jarosiewicz, N. Y. Masse, J. D. Simeral, J. Vogel, S. Haddadin, J. Liu, S. S. Cash, P. van der Smagt, and J. P. Donoghue. *Nature* **2012**, *485*, pp 372–375. doi: 10.1038/nature11076.
74. B. Wodlinger, J. E. Downey, E. C. Tyler-Kabara, A. B. Schwartz, M. L. Boninger, and J. L. Collinger. *J. Neural Eng.* **2015**, *12*(1), p 016011. doi: 10.1088/1741-2560/12/1/016011.
75. A. Mercanzini, P. Colin, J. C. Bensadoun, A. Bertsch, and P. Renaud. *IEEE Trans. Biomed. Eng.* **2009**, *56*(7), pp 1909–1918. doi: 10.1109/TBME.2009.2018457.
76. J. C. Williams, R. L. Rennaker, and D. R. Kipke. *Brain Res. Protocol.* **1999**, *4*(3), pp 303–313. doi: 10.1016/S1385-299X(99)00034-3.
77. R. W. Griffith and D. R. Humphrey. *Neurosci. Lett.* **2006**, *406*(1), pp 81–86. doi: 10.1016/j.neulet.2006.07.018.
78. D. Groupe and W. K. Cline. *IEEE Trans. Syst. Man Cybern. Syst.* **1975**, *267*, pp 252–259. doi: 10.1109/TSMC.1975.5408479.
79. T. A. Kuiken, L. A. Miller, R. D. Lipschutz, B. A. Lock, K. Stubblefield, P. D. Marasco, P. Zhou, and G. A. Dumanian. *Lancet* **2007**, *369*(9559), pp 371–380. doi: 10.1016/S0140-6736(07)60193-7.
80. B. Hudgins, P. Parker, and R. N. Scott. *IEEE Trans. Biomed. Eng.* **1993**, *40*(1), pp 82–94. doi: 10.1109/10.204774.
81. K. Englehart, B. Hudgins, P. A. Parker, and M. Stevenson. *Med. Eng. Phys.* **1999**, *21*(6), pp 431–438. doi: 10.1016/S1350-4533(99)00066-1.
82. J. L. Betthauser, C. L. Hunt, L. E. Osborn, M. R. Masters, G. Levay, R. R. Kaliki, and N. V. Thakor. *IEEE Trans. Biomed. Eng.* **2018**, *65*(4), pp 770–778. doi: 10.1109/TBME.2017.2719400.
83. T. Tsuji, O. Fukuda, M. Kaneko, and K. Ito. *Int. J. Adapt. Control Signal Process.* **2000**, *14*(8), pp 829–848.
84. L. J. Hargrove, E. J. Scheme, K. B. Englehart, and B. S. Hudgins. *IEEE Trans. Neural Syst. Rehabil. Eng.* **2010**, *18*(1), pp 49–57. doi: 10.1109/TNSRE.2009.2039590.
85. S. Amari and S. Wu. *Neural Netw.* **1999**, *12*(6), pp 783–789. doi: 10.1016/S0893-6080(99)00032-5.
86. H. C. Shin, V. Aggarwal, S. Acharya, M. H. Schieber, and N. V. Thakor. *IEEE Trans. Biomed. Eng.* **2010**, *57*(3), pp 754–760. doi: 10.1109/TBME.2009.2020791.
87. V. Gilja, P. Nuyujukian, C. A. Chestek, J. P. Cunningham, B. M. Yu, J. M. Fan, M. M. Churchland, M. T. Kaufman, J. C. Kao, S. I. Ryu, and K. V. Shenoy. *Nat. Neurosci.* **2012**, *15*(12), pp 1752–1757. doi: 10.1038/nn.3265.
88. C. Cipriani, C. Antfolk, M. Controzzi, G. Lundborg, B. Rosen, M. C. Carrozza, and F. Sebelius. *IEEE Trans. Neural Syst. Rehabil. Eng.* **2011**, *19*(3), pp 260–270. doi: 10.1109/TNSRE.2011.2108667.
89. M. Hauschild, G. H. Mulliken, I. Fineman, G. E. Loeb, and R. A. Andersen. *Proc. Natl. Acad. Sci. U. S. A.* **2012**, *109*(42), pp 17075–17080. doi: 10.1073/pnas.1215092109.
90. S. Acharya, F. Tenore, V. Aggarwal, R. Etienne-Cummings, M. H. Schieber, and N. V. Thakor. *IEEE Trans. Neural Syst. Rehabil. Eng.* **2008**, *16*(1), pp 15–23. doi: 10.1109/TNSRE.2007.916269.

91. K. Kahn, S. Saxena, E. Eskandar, N. Thakor, M. Schieber, J. T. Gale, B. Averbeck, U. Eden, and S. V. Sarma. *J. Neurosci. Methods* **2015**, *245*, pp 156–168. doi: 10.1016/j.jneumeth.2015.02.020.
92. R. Agarwal, N. V. Thakor, S. V. Sarma, and S. G. Massaquoi. *J. Neurosci.* **2015**, *35*(25), pp 9508–9525. doi: 10.1523/JNEUROSCI.2643-14.2015.
93. A. K. Bansal, W. Truccolo, C. E. Vargas-Irwin, and J. P. Donoghue. *J. Neurophysiol.* **2011**, *107*(5), pp 1337–1355. doi: 10.1152/jn.00781.2011.
94. A. Fougner, E. Scheme, A. D. C. Chan, K. Englehart, and Ø. Stavdahl. *IEEE Trans. Neural Syst. Rehabil. Eng.* **2011**, *19*(6), pp 644–651. doi: 10.1109/TNSRE.2011.2163529.
95. C. Cipriani, R. Sassu, M. Controzzi, and M. C. Carrozza. Influence of the Weight Actions of the Hand Prosthesis on the Performance of Pattern Recognition Based Myoelectric Control: Preliminary Study, in *Conf. Proc. IEEE Eng. Med. Biol. Soc. (EMBC)*, 2011; pp 1620–1623. doi: 10.1109/IEMBS.2011.6090468.
96. E. Scheme and K. Englehart. *J. Rehabil. Res. Dev.* **2011**, *48*(6), pp 643–659. doi: 10.1682/JRRD.2010.09.0177.
97. J. R. Wolpaw, D. J. McFarland, G. W. Neat, and C. A. Forneris. *Electroencephalogr. Clin. Neurophysiol.* **1991**, *78*(3), pp 252–259. doi: 10.1016/0013-4694(91)90040-B.
98. G. E. Fabiani, D. J. McFarland, J. R. Wolpaw, and G. Pfurtscheller. *IEEE Trans. Neural Syst. Rehabil. Eng.* **2004**, *12*(3), pp 331–338. doi: 10.1109/TNSRE.2004.834627.
99. J. R. Wolpaw, D. J. McFarland, and E. Bizzi. *Proc. Natl. Acad. Sci. U. S. A.* **2004**, *101*(51), pp 17849–17854. doi: 10.1073/pnas.0403504101.
100. F. Galán, M. Nuttin, E. Lew, P. W. Ferrez, G. Vanacker, J. Philips, and J. d. R. Millán. *Clin. Neurophysiol.* **2008**, *119*(9), pp 2159–2169. doi: 10.1016/j.clinph.2008.06.001.
101. A. Úbeda, J. M. Azorín, N. García, J. M. Sabater, and C. Pérez. Brain–Machine Interface Based on EEG Mapping to Control an Assistive Robotic Arm, in *Conf. Proc. IEEE Biomed. Robot. Biomechatron. (BioRob)*, June 2012; pp 1311–1315. doi: 10.1109/BioRob.2012.6290689.
102. E. C. Leuthardt, G. Schalk, J. R. Wolpaw, J. G. Ojemann, and D. W. Moran. *J. Neural Eng.* **2004**, *1*(2), pp 63–71. doi: 10.1088/1741-2560/1/2/001.
103. E. A. Felton, J. A. Wilson, J. C. Williams, and P. C. Garell. *J. Neurosurg.* **2007**, *106*(3), pp 495–500. doi: 10.3171/jns.2007.106.3.495.
104. G. Schalk, K. J. Miller, N. R. Anderson, J. A. Wilson, M. D. Smyth, J. G. Ojemann, D. W. Moran, J. R. Wolpaw, and E. C. Leuthardt. *J. Neural Eng.* **2008**, *5*(1), pp 75–84. doi: 10.1088/1741-2560/5/1/008.
105. S. Vadera, A. R. Marathe, J. Gonzalez-Martinez, and D. M. Taylor. *Neurosurg. Focus* **2013**, *34*(6), p E3. doi: 10.3171/2013.3.FOCUS1373.
106. W. Wang, J. L. Collinger, A. D. Degenhart, E. C. Tyler-Kabara, A. B. Schwartz, D. W. Moran, D. J. Weber, B. Wodlinger, R. K. Vinjamuri, R. C. Ashmore, J. W. Kelly, and M. L. Boninger. *PLoS One* **2013**, *8*(2), p e55344. doi: 10.1371/journal.pone.0055344.
107. T. A. Kuiken, G. Li, B. A. Lock, R. D. Lipschutz, L. A. Miller, K. A. Stubblefield, and K. B. Englehart. *JAMA* **2009**, *301*(6), pp 619–628. doi: 10.1001/jama.2009.116.
108. L. J. Hargrove, L. A. Miller, K. Turner, and T. A. Kuiken. *Sci. Rep.* **2017**, *7*(1). doi: 10.1038/s41598-017-14386-w.
109. D. Farina, I. Vujaklija, M. Sartori, T. Kapelner, F. Negro, N. Jiang, K. Bergmeister, A. Andalib, J. Principe, and O. C. Aszmann. *Nat. Biomed. Eng.* **2017**, *1*(2), p 25. doi: 10.1038/s41551-016-0025.
110. M. Ortiz-Catalan, B. Håkansson, and R. Brånemark. *Sci. Transl. Med.* **2014**, *6*(257), p 257re6. doi: 10.1126/scitranslmed.3008933.
111. S. Amsüss, P. M. Goebel, N. Jiang, B. Graimann, L. Paredes, and D. Farina. *IEEE Trans. Biomed. Eng.* **2014**, *61*(4), pp 1167–1176. doi: 10.1109/TBME.2013.2296274.
112. X. Zhu, J. Liu, D. Zhang, X. Sheng, and N. Jiang. *IEEE Trans. Neural Syst. Rehabil. Eng.* **2017**, *25*(3), pp 254–264. doi: 10.1109/TNSRE.2016.2562180.
113. D. P. McMullen, G. Hotson, K. D. Katyal, B. A. Wester, M. S. Fifer, T. G. McGee, A. Harris, M. S. Johannes, R. J. Vogelstein, and A. D. Ravitz. *IEEE Trans. Neural Syst. Rehabil. Eng.* **2014**, *22*(4), pp 784–796. doi: 10.1109/TNSRE.2013.2294685.
114. F. Clemente, S. Dosen, L. Lonini, M. Markovic, D. Farina, and C. Cipriani. *IEEE Trans. Hum.–Mach. Syst.* **2017**, *47*(4), pp 583–589. doi: 10.1109/THMS.2016.2611998.
115. R. P. Morse and E. F. Evans. *Nat. Med.* **1996**, *2*(8), pp 928–932. doi: 10.1038/nm0896-928.
116. B. S. Wilson and M. F. Dorman. *IEEE Sens. J.* **2008**, *8*(1), pp 131–147. doi: 10.1109/JSEN.2007.912917.
117. P. M. Lewis, H. M. Ackland, A. J. Lowery, and J. V. Rosenfeld. *Brain Res.* **2015**, *1595*, pp 51–73. doi: 10.1016/j.brainres.2014.11.020.
118. J. S. Pezaris and E. N. Eskandar. *Neurosurg. Focus* **2009**, *27*(1), p E6. doi: 10.3171/2009.4.FOCUS0986.
119. C. C. Della Santina, A. A. Migliaccio, and A. H. Patel. *IEEE Trans. Biomed. Eng.* **2007**, *54*(6), pp 1016–1030. doi: 10.1109/TBME.2007.894629.
120. J. A. Sabolich and G. M. Ortega. *J. Prosthet. Orthot.* **1994**, *6*(2), pp 36–41.
121. G. Q. Zhao, Y. Zhang, M. A. Hoon, J. Chandrashekar, I. Erlenbach, N. J. P. Ryba, and C. S. Zuker. *Cell* **2003**, *115*(3), pp 255–266. doi: 10.1016/S0092-8674(03)00844-4.
122. A. Kumari, A. N. Ermilov, M. Grachtchouk, A. A. Dlugosz, B. L. Allen, R. M. Bradley, and C. M. Mistretta. *Proc. Natl. Acad. Sci. U. S. A.* **2017**, *114*(48), p E10378. doi: 10.1073/pnas.1712881114.
123. K. Kollndorfer, K. Kowalczyk, E. Hoche, C. A. Mueller, M. Pollak, S. Trattnig, and V. Schöpf. *Neural Plast.* **2014**, *2014*, p 140419. doi: 10.1155/2014/140419.
124. D. H. Coelho and R. M. Costanzo. *Otolaryngol. Head Neck Surg.* **2016**, *155*(3), pp 526–532. doi: 10.1177/0194599816646358.
125. R. Costanzo and D. Coelho. Olfactory implant system. U.S. Patent 9517342B2, December 13, 2016.
126. R. Costanzo, M. Sabot, W. Yeo, and G. Allen. Wireless implantable taste system. U.S. Patent 20170087363A1, March 2017.
127. National Institutes of Health and National Institute on Deafness and Other Communication Disorders (NIDCD). Cochlear Implants. Available at https://www.nidcd.nih.gov/health/cochlear-implants, October 20, 2017.
128. Z. Su, J. A. Fishel, T. Yamamoto, and G. E. Loeb. *Front. Neurorobot.* **2012**, *6*(7). doi: 10.3389/fnbot.2012.00007.
129. R. S. Armiger, F. V. Tenore, K. D. Katyal, M. S. Johannes, A. Makhlin, M. L. Natter, J. E. Colgate, S. J. Bensmaia, and R. J. Vogelstein. *Johns Hopkins APL Tech. Dig.* **2013**, *31*(4), pp 345–353.

130. L. Osborn, W. W. Lee, R. Kaliki, and N. Thakor. Tactile Feedback in Upper Limb Prosthetic Devices Using Flexible Textile Force Sensors, in *Conf. Proc. IEEE Biomed. Robot. Biomechatron. (BioRob)*, 2014; pp 114–119. doi: 10.1109/BIOROB.2014.6913762.
131. S. S. Hsiao and M. Gomez-Ramirez. In *Handbook of Psychology, vol. 3: Behavioral Neuroscience*, 2nd ed.; Weiner, I. B.; Nelson, R. J.; Mizumori, S., Eds.; Wiley: Hoboken, NJ, 2012; pp 206–239.
132. R. S. Johansson and K. J. Cole. *Curr. Opin. Neurobiol.* **1992**, *2*(6), pp 815–823. doi: 10.1016/0959-4388(92)90139-C.
133. V. Abraira and D. Ginty. *Neuron* **2013**, *79*(4), pp 618–639. doi: 10.1016/j.neuron.2013.07.051.
134. J. A. Fishel and G. E. Loeb. Sensing Tactile Microvibrations with the BioTac – Comparison with Human Sensitivity, in *Conf. Proc. IEEE Biomed. Robot. Biomechatron. (BioRob)*, 2012; pp 1122–1127. doi: 10.1109/BioRob.2012.6290741.
135. B. Delhaye, P. Lefèvre, and J. Thonnard. *J. R. Soc. Interface* **2014**, *11*(100). doi: 10.1098/rsif.2014.0698.
136. H. P. Saal, B. P. Delhaye, B. C. Rayhaun, and S. J. Bensmaia. *Proc. Natl. Acad. Sci. U. S. A.* **2017**, *114*(28), p E5702. doi: 10.1073/pnas.1704856114.
137. A. Perez Fornos, N. Guinand, R. van de Berg, R. Stokroos, S. Micera, H. Kingma, M. Pelizzone, and J. Guyot. *Front. Neurol.* **2014** *5*(66). doi: 10.3389/fneur.2014.00066.
138. T. Z. Lauritzen, J. Harris, S. Mohand-Said, J. Sahel, J. Dorn, K. McClure, and R. Greenberg. *Front. Neurosci.* **2012** *6*(168). doi: 10.3389/fnins.2012.00168.
139. J. Golub, L. Ling, K. Nie, A. Nowack, S. Shepherd, S. Bierer, E. Jameyson, C. Kaneko, J. Phillips, and J. Rubinstein. *Otol. Neurotol.* **2014**, *35*(1), pp 136–147. doi: 10.1097/MAO.0000000000000003.
140. X. Sui, L. Li, X. Chai, K. Wu, C. Zhou, X. Sun, X. Xu, X. Li, and Q. Ren. In *Implantable Neural Prostheses 1*; Greenbaum, E.; Zhou, D., Eds.; Springer US: New York, 2009; pp 43–83.
141. W. H. Dobelle, M. G. Mladejovsky, and J. P. Girvin. *Science* **1974**, *183*(4123), pp 440–444. doi: 10.1126/science.183.4123.440.
142. T. S. Davis, H. A. C. Wark, D. T. Hutchinson, D. J. Warren, K. O'Neill, T. Scheinblum, G. A. Clark, R. A. Normann, and B. Greger. *J. Neural Eng.* **2016**, *13*(3), p 036001. doi: 10.1088/1741-2560/13/3/036001.
143. M. M. Merzenich, R. J. Nelson, M. P. Stryker, M. S. Cynader, A. Schoppmann, and J. M. Zook. *J. Comp. Neurol.* **1984**, *224*(4), pp 591–605. doi: 10.1002/cne.902240408.
144. F. Vega-Bermudez and K. O. Johnson. *Brain* **2002**, *125*(6), pp 1256–1264. doi: 10.1093/brain/awf129.
145. T. R. Makin and S. J. Bensmaia. *Trends Cogn. Sci.* **2017**, *21*(3), pp 195–204. doi: 10.1016/j.tics.2017.01.002.
146. S. Wendelken, D. M. Page, T. Davis, H. A. C. Wark, D. T. Kluger, C. Duncan, D. J. Warren, D. T. Hutchinson, and G. A. Clark. *J. Neuroeng. Rehabil.* **2017**, *14*(1), p 121. doi: 10.1186/s12984-017-0320-4.
147. L. Osborn, M. Fifer, C. Moran, J. Betthauser, R. Armiger, R. Kaliki, and N. Thakor. Targeted Transcutaneous Electrical Nerve Stimulation for Phantom Limb Sensory Feedback, in *Conf. Proc. IEEE Biomed. Circuits Syst. (BioCAS)*, 2017; pp 1–4. doi: 10.1109/BIOCAS.2017.8325200.
148. F. Zeng. *Trends Amplif.* **2004**, *8*(1), pp 1–34. doi: 10.1177/108471380400800102.
149. G. S. G. Géléoc and J. R. Holt. *Science* **2014**, *344*(6184), p 1241062. doi: 10.1126/science.1241062.
150. H. Skarzynski, A. Lorens, A. Piotrowska, and I. Anderson. *Acta Otolaryngol.* **2007**, *127*(1), pp 41–48. doi: 10.1080/00016480500488917.
151. B. S. Wilson, C. C. Finley, D. T. Lawson, R. D. Wolford, D. K. Eddington, and W. M. Rabinowitz. *Nature* **1991**, *352*(6332), pp 236–238. doi: 10.1038/352236a0.
152. B. S. Wilson, C. C. Finley, D. T. Lawson, R. D. Wolford, and M. Zerbi. *J. Rehabil. Res. Dev.* **1993**, *30*(1), pp 110–116.
153. Z. M. Smith, B. Delgutte, and A. J. Oxenham. *Nature* **2002**, *416*(6876), pp 87–90. doi: 10.1038/416087a.
154. B. S. Wilson, R. Schatzer, E. A. Lopez-Poveda, X. Sun, D. T. Lawson, and R. D. Wolford. *Ear Hear.* **2005**, *26*(4), p 81S.
155. K. Gfeller, C. Turner, J. Oleson, X. Zhang, B. Gantz, R. Froman, and C. Olszewski. *Ear Hear.* **2007**, *28*(3), pp 412–423. doi: 10.1097/AUD.0b013e3180479318.
156. J. Rouger, S. Lagleyre, B. Fraysse, S. Deneve, O. Deguine, and P. Barone. *Proc. Natl. Acad. Sci. U. S. A.* **2007**, *104*(17), pp 7295–7300. doi: 10.1073/pnas.0609419104.
157. M. H. Maghami, A. M. Sodagar, A. Lashay, H. Riazi-Esfahani, and M. Riazi-Esfahani. *J. Ophthalmic Vis. Res.* **2014**, *9*(4), pp 494–505. doi: 10.4103/2008-322X.150830.
158. E. D. Cohen. *J. Neural Eng.* **2007**, *4*(2), p 14. doi: 10.1088/1741-2560/4/2/R02.
159. S. V. Hiremath, E. C. Tyler-Kabara, J. J. Wheeler, D. W. Moran, R. A. Gaunt, J. L. Collinger, S. T. Foldes, D. J. Weber, W. Chen, M. L. Boninger, and W. Wang. *PLoS One* **2017**, *12*(5), p e0176020. doi: 10.1371/journal.pone.0176020.
160. S. Raspopovic, M. Capogrosso, F. M. Petrini, M. Bonizzato, J. Rigosa, G. Di Pino, J. Carpaneto, M. Controzzi, T. Boretius, E. Fernandez, G. Granata, C. M. Oddo, L. Citi, A. L. Ciancio, C. Cipriani, M. C. Carrozza, W. Jensen, E. Guglielmelli, T. Stieglitz, P. M. Rossini, and S. Micera. *Sci. Transl. Med.* **2014**, *6*(222), p 222ra19. doi: 10.1126/scitranslmed.3006820.
161. E. D'Anna, F. M. Petrini, F. Artoni, I. Popovic, I. Simanić, S. Raspopovic, and S. Micera. *Sci. Rep.* **2017**, *7*(1), p 10930. doi: 10.1038/s41598-017-11306-w.
162. E. L. Graczyk, M. A. Schiefer, H. P. Saal, B. P. Delhaye, S. J. Bensmaia, and D. J. Tyler. *Sci. Transl. Med.* **2016**, *8*(362), p 362ra142. doi: 10.1126/scitranslmed.aaf5187.
163. C. Antfolk, M. D'Alonzo, M. Controzzi, G. Lundborg, B. Rosen, F. Sebelius, and C. Cipriani. *IEEE Trans. Neural Syst. Rehabil. Eng.* **2013**, *21*(1), pp 112–120. doi: 10.1109/TNSRE.2012.2217989.
164. M. D'Alonzo, F. Clemente, and C. Cipriani. *IEEE Trans. Neural Syst. Rehabil. Eng.* **2015**, *23*(3), pp 450–457. doi: 10.1109/TNSRE.2014.2337952.
165. G. L. Breschi, C. Ciliberto, T. Nieus, L. Rosasco, S. Taverna, M. Chiappalone, and V. Pasquale. *Comput. Intell. Neurosci.* **2015**, *2015*, p e359590. doi: 10.1155/2015/359590.
166. M. K. Balasubramaniam, A. S. Chidambaranathan, G. Shanmugam, and R. Tah. *J. Clin. Diagn. Res.* **2016**, *10*(2), p ZE04. doi: 10.7860/JCDR/2016/15868.7184.
167. N. Guinand, R. van de Berg, S. Cavuscens, R. J. Stokroos, M. Ranieri, M. Pelizzone, H. Kingma, J. P. Guyot, and A. Perez-Fornos. *ORL J. Otorhinolaryngol. Relat. Spec.* **2015**, *77*(4), pp 227–240. doi: 10.1159/000433554.
168. M. Schiefer, D. Tan, S. M. Sidek, and D. J. Tyler. *J. Neural Eng.* **2015**, *13*(1), p 016001. doi: 10.1088/1741-2560/13/1/016001.
169. P. D. Marasco, J. S. Hebert, J. W. Sensinger, C. E. Shell, J. S. Schofield, Z. C. Thumser, R. Nataraj, D. T. Beckler, M. R. Dawson, D. H. Blustein, S. Gill, B. D. Mensh, R. Granja-Vazquez, M. D. Newcomb, J. P. Carey, and B. M.

Orzell. *Sci. Transl. Med.* **2018**, *10*(432), p eaao6990. doi: 10.1126/scitranslmed.aao6990.

170. L. Osborn, R. R. Kaliki, A. B. Soares, and N. V. Thakor. *IEEE Trans. Haptics* **2016**, *9*(2), pp 196–206. doi: 10.1109/TOH.2016.2564965.
171. E. M. Izhikevich. *IEEE Trans. Neural Netw.* **2003**, *14*(6), pp 1569–1572. doi: 10.1109/TNN.2003.820440.
172. Y. Dong, S. Mihalas, S. S. Kim, T. Yoshioka, S. Bensmaia, and E. Niebur. *J. Neurophysiol.* **2013**, *109*(5), pp 1350–1359. doi: 10.1152/jn.00395.2012.
173. L. Osborn, H. Nguyen, R. Kaliki, and N. Thakor. Prosthesis Grip Force Modulation Using Neuromorphic Tactile Sensing, in *Proc. Myoelec. Controls Symp*., 2017; pp 188–191.
174. C. M. Oddo, S. Raspopovic, F. Artoni, A. Mazzoni, G. Spigler, F. Petrini, F. Giambattistelli, F. Vecchio, F. Miraglia, L. Zollo, G. Di Pino, D. Camboni, M. C. Carrozza, E. Guglielmelli, P. M. Rossini, U. Faraguna, and S. Micera. *elife* **2016**, *5*, p e09148. doi: 10.7554/eLife.09148.
175. B. C. K. Tee, A. Chortos, A. Berndt, A. K. Nguyen, A. Tom, A. McGuire, Z. C. Lin, K. Tien, W. Bae, H. Wang, P. Mei, H. Chou, B. Cui, K. Deisseroth, T. N. Ng, and Z. Bao. *Science* **2015**, *350*(6258), pp 313–316. doi: 10.1126/science.aaa9306.
176. L. Osborn, H. Nguyen, J. Betthauser, R. Kaliki, and N. Thakor. Biologically Inspired Multi-layered Synthetic Skin for Tactile Feedback in Prosthetic Limbs, in *Conf. Proc. IEEE Eng. Med. Biol. Soc. (EMBC)*, 2016; pp 4622–4625. doi: 10.1109/EMBC.2016.7591757.
177. B. C. Tee, C. Wang, R. Allen, and Z. Bao. *Nat. Nanotechnol.* **2012**, *7*(12), pp 825–832. doi: 10.1038/nnano.2012.192.
178. S. Terryn, J. Brancart, D. Lefeber, G. Van Assche, and B. Vanderborght. *Sci. Robot.* **2017**, *2*(9), p eaan4268. doi: 10.1126/scirobotics.aan4268.
179. A. Chortos, J. Liu, and Z. Bao. *Nat. Mater.* **2016**, *15*(9), pp 937–950. doi: 10.1038/nmat4671.

LUKE E. OSBORN
Department of Biomedical Engineering, Johns Hopkins School of Medicine, Baltimore, MD, USA

JOSEPH L. BETTHAUSER
Department of Electrical and Computer Engineering, Johns Hopkins University, Baltimore, MD, USA

NITISH V. THAKOR
Department of Biomedical Engineering, Johns Hopkins School of Medicine, Baltimore, MD, USA

Department of Electrical and Computer Engineering, Johns Hopkins University, Baltimore, MD, USA

Singapore Institute for Neurotechnology, National University of Singapore, Singapore